

Journal: ACP

Title: Photochemical aging of volatile organic compounds associated with oil and natural gas extraction in the Uintah Basin, UT, during a wintertime ozone formation event

Author(s): A. R. Koss, J. de Gouw, C. Warneke, J. B. Gilman, B. M. Lerner, M. Graus, B. Yuan, P. Edwards, S. S. Brown, R. Wild, J. M. Roberts, T. S. Bates, and P. K. Quinn

MS No.: acp-2015-89

MS Type: Research Article

Special Issue: Uintah Basin Winter Ozone Studies (ACP/AMT Inter-Journal SI)

Reply to reviewers

We thank the reviewers for their comments. Below we respond to reviewer comments and describe revisions to the manuscript.

Reviewer 1.

Koss et al. present comprehensive wintertime ground VOC concentration measurements and analysis near oil and natural gas extraction activities in the Uintah Basin, UT. Among others, VOC ratios to benzene are used to characterize and discriminate the sources (gas, oil). From the observed VOC concentrations emission or formation rates are estimated using fits of VOC:benzene ratios as a function of time, relying on different assumptions. These ratios are also used to explain oxygenated VOC production and loss via OH chemistry, photolysis, and primary emission. Basin wide extrapolation of benzene emission rate to basin wide methane emission rate was done and showed similar value observed earlier from aircraft. Based on the carbon budget analysis using two independent approaches the authors conclude that a significant missing source must exist in primary emission which is unaccounted for. The OH rate constants were derived for C8, C9 and C10 aromatics in this study. Calculated daily OH concentrations were constrained from actinic flux and VOC concentrations, and agreed well with those from MCM. The data look consistent and of high quality, and proposed analyses seem particularly advantageous because of their simplicity. In summary, these observations are novel and have an important significance elucidating atmospheric impacts from the oil and gas extraction practices, clearly associated with high VOCs and ozone formation events. I therefore would like to highly recommend this paper for publication in ACP, if the following (relatively minor) comments can be addressed:

1. The authors did an excellent job presenting the useful and extremely comprehensive observations of VOCs. I am further wondering if any sulfur containing hydrocarbons such as sulfides (e.g. DMS, DES) or thiols (e.g. methanethiol, ethanethiol) were observed or if they could deserve some attention, given that a variety of sulfur containing hydrocarbons is expected from sour oil and gas (Hammer et al., 2006) and that substantial concentrations of hydrogen sulfide were earlier reported from the same missions (Li et al., 2014).

Response:

Sulfur-containing species are certainly very interesting from an emissions and air toxics perspective. We have limited observations from a PTR-ToF instrument operated in 2013 (Warneke et al., 2015) that could provide information on sulfur-containing hydrocarbons. However, interpretation of these data would require a great deal of further work and analysis of these species is better suited to a separate manuscript.

We can respond as to whether these species would likely have a significant impact on the carbon budget described in section 4. From Li's work (Li et al., 2014), we know that H₂S was present at an average mixing ratio of 0.6ppbv and was typically under 2 ppbv. These concentrations are significant, especially considering the toxicity of H₂S, but are small compared to mixing ratios of

hydrocarbons. From previous work by other research teams, we know that H₂S is typically the dominant reduced sulfur-containing gas phase species in oil and gas producing regions (Tarver and Dasgupta, 1997). Organic mercaptan species, if present, likely had even smaller concentrations than H₂S. These species could still play important roles in air quality and oxidation chemistry, but it is unlikely they contributed significantly to carbon mass budget.

To recognize the possible presence of sulfur species we have added a reference to Li et al. (2014) at Page 6406 line 8, and have added “Some sulfur-containing species were measured (Li et al., 2014) but are not discussed in this manuscript” at Page 6408 Line 29.

2. Methanol was observed in extremely high mixing ratios (up to 200 ppbv) clearly pointing to its primary emission source dominating the site (p.6420 L3-5). Table 1 shows very high methanol average mixing ratio (44.9 ppbv) but places methanol in secondary rather than in primary sources. This might mislead some readers to think that these high concentrations of methanol are mostly of the photochemical origin. Including the primary term in Eq. 6 did not result in a good fit from the OVOC analysis, so does the upper limit of the photochemical methanol carbon mass not seem exaggerated (Figure 10)?

3. Consequently, could it not be more reasonable to present methanol as mostly primary compound since the beginning of the story? In addition, it could make it more clear, if methanol was included in primary, or both primary and secondary sources (or in a third mixed category) in Table 1.

Response (to 2 and 3):

We have added additional explanation to clarify the possible sources of methanol and formaldehyde.

First, in table 1, we have placed methanol and formaldehyde in a third mixed/undetermined source category as suggested.

Second, we have moved Line 17, Page 6409 (“C6-C10 aromatic VOCs were selected for analysis of primary compounds because they have readily identifiable parent masses, they are sensitively detected by PTR-MS, and have a relatively wide range of reactivity with OH ($k_{OH} = 1.22 \times 10^{-12} \text{ s}^{-1}$ to $56 \times 10^{-12} \text{ s}^{-1}$)”) to Page 6411, Line 19 to clarify which VOCs were included in analysis of primary compounds, and why.

Third, on Page 6418, we have revised paragraph 1 to read, “We also assume that the only source of these species is photochemistry; i.e. they are not emitted directly from primary sources. **Methanol and formaldehyde are included in this section as they are oxygenated species. However, the high observed mixing ratios of methanol and formaldehyde (Table 1), previous modeling work (Edwards et al., 2014), and knowledge of industry practices indicates that these two species also have direct (primary) sources. We first analyzed methanol and formaldehyde assuming solely photochemical sources, to investigate the extent to which secondary formation can explain their behavior. We then modified the analysis to consider primary emission of these species.** Methanol and formaldehyde are discussed separately in the analysis (below).” (New content in bold text.)

Fourth, we have split Figure 9 into two panels, to better provide visual distinction between the two groups of compounds, and have updated the caption to read, “The best fit does not reproduce night time variability or trends in methanol and formaldehyde, which may have substantial primary sources uncorrelated with benzene.”

Finally, we have edited Page 6420 lines 1-5 to clarify that methanol clearly has primary sources. Line 1-2 now reads, “For methanol, this behavior is almost certainly due to large primary sources.” Line 3 now clearly states that methanol is used by industry on wellpads. We have added “It is therefore unsurprising that methanol variation is poorly described by Equation (6)” before line 6. We also briefly describe the relationship between formaldehyde and NO_x at line 9 (see response to Reviewer 2).

These revisions, together with the extant discussion of primary emission of methanol and formaldehyde (Page 6420 paragraph 1), clarify our analysis of the sources of these two compounds

We address the reviewer's concern regarding an exaggerated methanol contribution to photochemical carbon mass in our response to point 4 (below).

4. Further on methanol, how would the inclusion of methanol to primary or secondary (or primary+secondary) compounds affect the total carbon mass balance?

Response: We agree with the reviewer that the classification of methanol and formaldehyde as primary or secondary has an effect on the total carbon mass balance. We have constrained this effect by including some additional calculation in the manuscript. We have inserted the following paragraph on Page 6422, after Line 20:

"Methanol and formaldehyde have substantial primary sources, so including them in this calculation artificially increases the percentage of secondary species accounted for: 0.64×10^{-10} gram C cm^{-3} is an upper bound to the mass of measured secondary species. If we assume methanol is entirely primary, measured secondary species only sum to 0.48×10^{-10} gram C cm^{-3} , or 12.9% of calculated secondary carbon mass. If we assume both methanol and formaldehyde have no photochemical sources, measured secondary species sum to 0.46×10^{-10} gram C cm^{-3} , or 12.5% of calculated secondary carbon mass. Figure 10 shows the upper bound to measured secondary species (including both methanol and formaldehyde)."

5. Figure 10. Could "start of ozone event: measured oxygenates" be also zoomed in to show the carbon mass broken down by individual compounds?

Response: We added an additional inset in Figure 10 to show speciation of oxygenates as suggested.

6. Figure 8, the pie chart shows C2-C5 alkanes and methane but the caption indicates that C1-C5 alkanes contributed significantly to OH reactivity. It may seem a little bit confusing because C1 (methane) is shown to have a relatively small contribution.

Response: The reviewer is correct in understanding that C1 (methane) did not contribute significantly to OH reactivity, compared to other alkanes. We have corrected this error in the caption, and corrected Page 6418 Line 21-24 to read "Despite how slowly these compounds react with OH, the very large concentration of these compounds means that C2-C5 alkanes account for most of the reactions between OH and VOCs, and are the most important precursor compounds (Fig. 8b)."

References:

Li, R., Warneke, C., Graus, M., Field, R., Geiger, F., Veres, P. R., Soltis, J., Li, S.-M., Murphy, S. M., Sweeney, C., Pétron, G., Roberts, J. M., and de Gouw, J.: Measurements of hydrogen sulfide (H₂S) using PTR-MS: calibration, humidity dependence, inter-comparison and results from field studies in an oil and gas production region, *Atmos. Meas. Tech.*, 7, 3597-3610, doi:10.5194/amt-7-3597-2014, 2014.

Tarver, G. A. and Dasgupta, P. K.: Oil Field Hydrogen Sulfide in Texas: Emission Estimates and Fate, *Environ. Sci. Technol.*, 31, 3669-3676, 1997.

Warneke, C., Veres, P., Murphy, S. M., Soltis, J., Field, R. A., Graus, M. G., Koss, A., Li, S.-M., Li, R., Yuan, B., Roberts, J. M., and de Gouw, J. A.: PTR-QMS versus PTR-TOF comparison in a region with oil and natural gas extraction industry in the Uintah Basin in 2013, *Atmos. Meas. Tech.*, 8, 411-420, doi:10.5194/amt-8-411-2015, 2015.

Reviewer 2.

The study conducted by Koss et. al. on the photochemical aging of volatile organic compounds in the Uintah Basin during a high ozone event utilizes the stagnant conditions to assume mixing into or out of the Basin is not occurring. These high ozone events in the wintertime conditions in the Uintah Basin are producing levels that rival the highest summertime urban ozone levels observed in the United States. The authors utilize the stagnant conditions and their measurements of aromatics and VOCs to, in part, determine emission rates from oil and gas operations, estimate OH concentrations, and estimate the mass budget of secondary products. I recommend this paper for publication in ACP with the following minor comments/thoughts:

1. Reading through the paper left me wanting to know more about the observed levels of other compounds. A description or plot of the NO_x levels would help further identify the conditions along with developing an understanding of combustion sources in the Basin. Formaldehyde and methanol were shown to have primary emission sources and interested if the NO_x correlates with the diurnal formaldehyde observations. The techniques used in the paper with additional measurements might help distinguish the secondary, combustion, or non-combustion related (methanol degradation in well fluids) sources of formaldehyde.

Response: We have added a time series showing NO_x concentrations to Figure 1. There is not an obvious correlation between formaldehyde and NO_x, and we have added a line stating this at Page 6420 Line 9. More research is needed to understand the relative primary and secondary sources of formaldehyde. This discussion may be worth a separate manuscript, especially considering formaldehyde's prominent role as a radical precursor.

2. The simplicity of this technique relies on dominant reaction pathways of aromatics with OH. On page 6409, line 21, a sentence might clarify the elimination of other sinks from ozone and NO₃.

Response: We have added the line, "Additionally, reaction rates of the primary species considered here (C6-C10 aromatics) with O₃ and NO₃ are at least several orders of magnitude lower than reaction rates with OH (Atkinson and Arey, 2003)," at Page 6411 Line 1.

Revised Figures

Figure 09

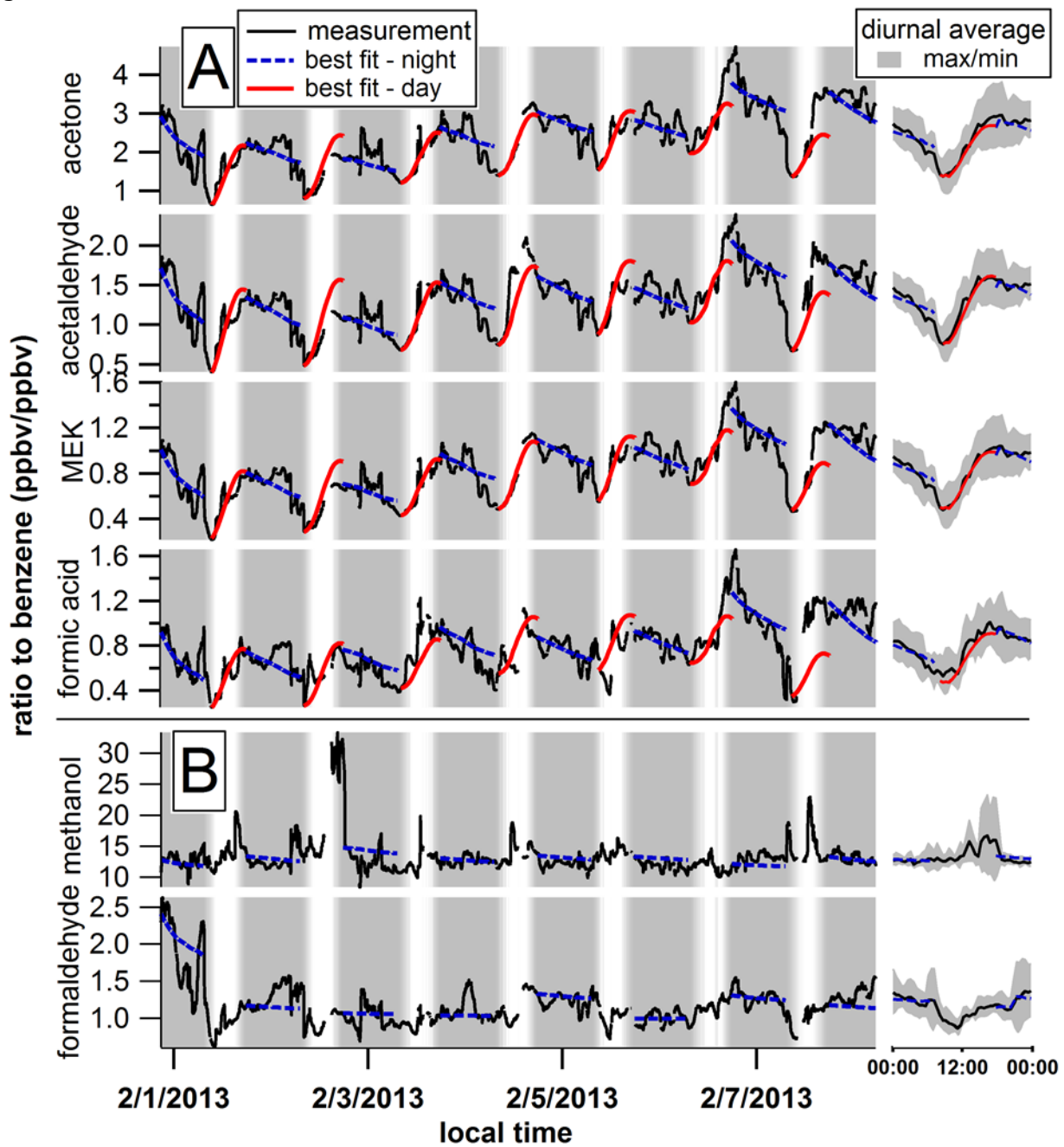
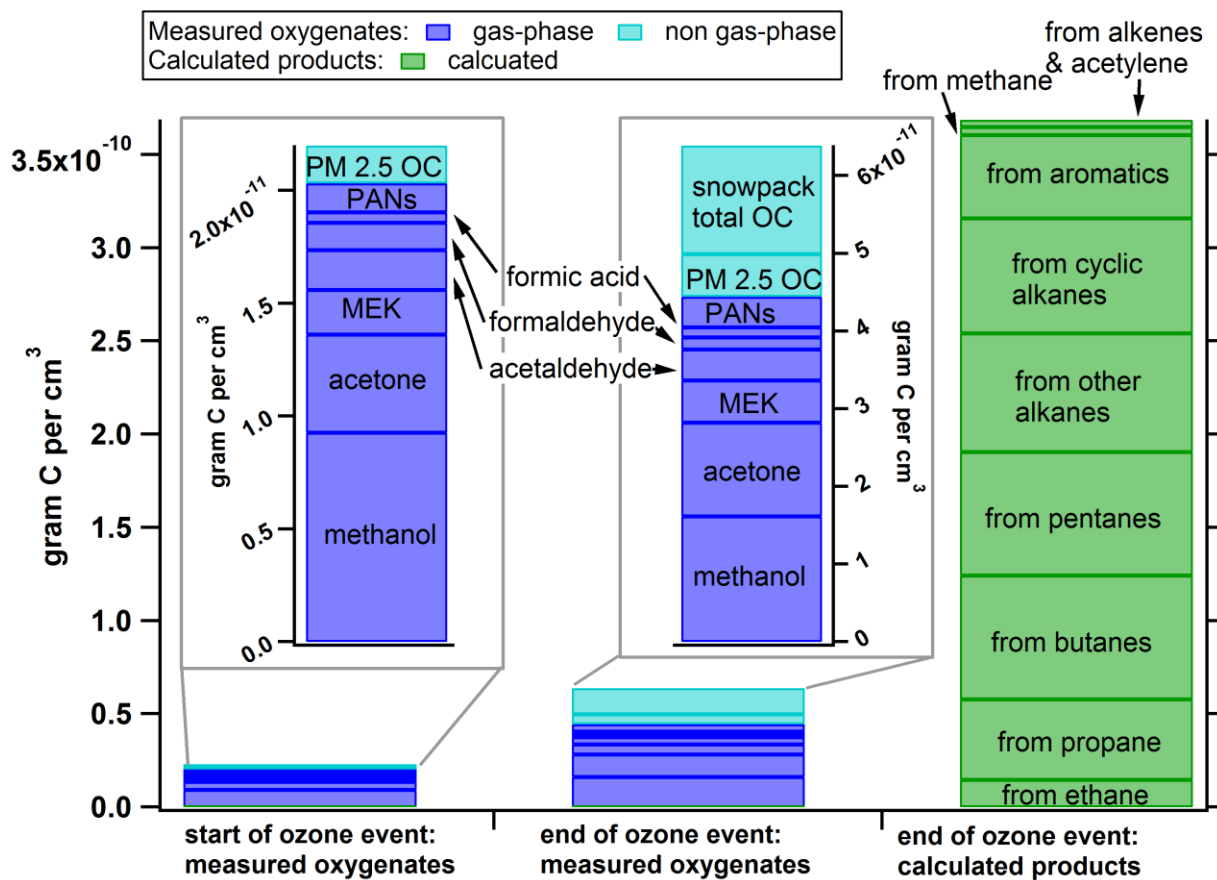


Figure 10



1 **Photochemical aging of volatile organic compounds associated with oil and natural gas**
2 **extraction in the Uintah Basin, UT, during a wintertime ozone formation event**

3
4 **A. R. Koss^{1,2}, J. de Gouw^{1,2}, C. Warneke^{1,2}, J. B. Gilman^{1,2}, B. M. Lerner^{1,2}, M. Graus^{1,2,*}, B.**
5 **Yuan^{1,2}, P. Edwards^{1,2,†}, S. S. Brown², R. Wild^{1,2}, J. M. Roberts², T. S. Bates^{3,4}, P. K. Quinn⁴**

6
7 [1]{Cooperative Institute for Research in Environmental Sciences, Univ. of Colorado, Boulder,
8 CO, USA}

9 [2]{NOAA Earth System Research Laboratory, Chemical Sciences Division, Boulder, CO, USA}

10 [3]{Joint Institute for the Study of the Atmosphere and Ocean, University of Washington, Seattle,
11 WA}

12 [4]{NOAA/Pacific Marine Environmental Laboratory, Seattle, WA}

13 [*]{now at: Institute of Meteorology and Geophysics, Innsbruck University, Innsbruck, Austria}

14 [†]{now at: Department of Chemistry, University of York, York, YO10 5DD, UK}

15 Correspondence to: A. R. Koss (abigail.koss@noaa.gov)

16

17 **Abstract**

18 High concentrations of volatile organic compounds (VOCs) associated with oil and natural gas
19 extraction were measured during a strong temperature inversion in winter of 2013 at a rural site in
20 the Uintah Basin, Utah. During this period, photochemistry enhanced by the stagnant
21 meteorological conditions and concentrated VOCs led to high ozone mixing ratios (150ppbv). A
22 simple analysis of aromatic VOCs measured by proton-transfer-reaction mass-spectrometry (PTR-
23 MS) is used to estimate (1) VOC emission ratios (the ratio of two VOCs at the time of emission)
24 relative to benzene, (2) aromatic VOC emission rates, and (3) ambient OH radical concentrations.
25 These quantities are determined from a best fit to VOC:benzene ratios as a function of time. The
26 main findings are that (1) emission ratios are consistent with contributions from both oil and gas
27 producing wells; (2) the emission rate of methane ($27\text{-}57 \times 10^3$ kg methane hr^{-1}), extrapolated from
28 the emission rate of benzene ($4.1 \pm 0.4 \times 10^5$ molecules $\text{cm}^{-3} \text{s}^{-1}$), agrees with an independent estimate
29 of methane emissions from aircraft measurements in 2012; and (3) calculated daily OH
30 concentrations are low, peaking at 1×10^6 molecules cm^{-3} , and are consistent with Master Chemical
31 Mechanism (MCM) modeling. The analysis is extended to photochemical production of

32 oxygenated VOCs measured by PTRMS and is able to explain daytime variability of these species.
33 It is not able to completely reproduce nighttime behavior, possibly due to surface deposition. Using
34 results from this analysis, the carbon mass of secondary compounds expected to have formed by
35 the sixth day of the stagnation event was calculated, then compared to the measured mass of
36 primary and secondary compounds. Only 17% of the expected secondary carbon mass is accounted
37 for by gas phase, aerosol, and snow organic carbon measurements. The disparity is likely due to
38 substantial amounts of unquantified oxygenated products.

39

40 **1. Introduction**

41 Natural gas, crude oil, and natural gas liquids are major fuel sources -- accounting for 54% of 2013
42 US domestic energy production -- and extraction of these resources has been rising substantially
43 since the mid 2000's (US Energy Information Administration, 2014). This activity is associated
44 with a range of possible environmental issues. Emissions due to extraction can: increase
45 atmospheric concentrations of methane, a greenhouse gas (Miller et al., 2013; Brandt et al., 2014);
46 directly impact local air quality through release of air toxics (Moore et al., 2014; Adgate et al.,
47 2014; [Li et al., 2014](#)); and contribute to photochemical ozone formation (Schnell et al., 2009;
48 Edwards et al., 2014; Carter and Seinfeld, 2012). Many scientific aspects of these processes are
49 uncertain. Emissions budgets of methane and other VOCs are poorly constrained and frequently
50 do not agree with inventory estimates (Brandt et al., 2014; Miller et al., 2013). Many variables can
51 affect the composition of emissions, including well life-cycle stage, extraction techniques, whether
52 the well is producing oil or gas, and diverse infrastructure/equipment components (Moore et al.,
53 2014; Litovitz et al., 2013; Allen et al., 2013). Wintertime ozone events, while sharing some
54 similarities with ozone formation typically seen in urban areas during the summer, occur in
55 different meteorological and chemical conditions and have attracted several recent measurement
56 and modeling investigations (Schnell et al., 2009; Kotamarthi and Holdridge, 2007; Carter and
57 Seinfeld, 2012; Edwards et al., 2013; Edwards et al., 2014).

58

59 The Uintah Basin, located in northeastern Utah, is a region of intense oil and natural gas extraction
60 activity. Approximately 4000 active oil-producing and 6500 gas-producing wells are located in a
61 10000 km² area, with an additional 1000 wells added each year (Utah Oil and Gas, 2014). In
62 January and February of 2012-2014, a suite of chemical and meteorological instrumentation was

63 deployed at Horse Pool, a remote site in the eastern part of the basin. Little active photochemistry
64 was observed in 2012, but in 2013 ground snow cover was accompanied by several sustained
65 periods of strong temperature inversion. Temperature inversions trap ozone precursors emitted by
66 oil and natural gas activity (VOCs and NO_x) and ozone close to the surface. Increased actinic flux
67 from reflective snow cover contributes to heightened ozone-producing photochemistry (Edwards,
68 2014). The gradual buildup of VOCs and ozone during a several day period of these conditions
69 can lead to very high mixing ratios – in this case, up to 5ppmC non-methane hydrocarbon and
70 150ppb ozone. VOCs are a fundamental component of the photochemistry that occurred during
71 these events, and so it is important to quantify (1) the rate at which VOCs are emitted from primary
72 sources (“emission rate”), (2) the source composition of the VOC mixture (“emission ratios”), and
73 (3) the degree of VOC oxidation.

74
75 In this paper, we analyze the photochemical aging of VOCs during an ozone formation period in
76 2013. We first examine primary, aromatic VOCs with a method that considers reaction with OH
77 and constant primary emission. This analysis provides information on the emission rate and
78 emission ratios of these VOCs, and the typical daily concentration of OH. We next investigate
79 oxygenated VOCs with a method that includes production and loss via OH chemistry and loss to
80 photolysis. This approach identifies oxygenated VOCs with substantial primary sources and
81 suggests rates of carbonyl formation from photochemistry. Finally, we calculate the organic carbon
82 mass balance of primary and product species. This defines overall VOC speciation and determines
83 the fraction of product species measured with the Horse Pool instrumentation.

84

85 **2. Methods**

86 **2.1 Measurement site and instrumentation.**

87 The Horse Pool site is located in the central eastern part of the Uintah basin, approximately 30km
88 south of Vernal, Utah. Meteorological, gas, and particle-phase measurements were deployed
89 concurrently at the site from 15 Jan. - 29 Feb. 2012, 23 Jan. – 22 Feb. 2013, and 15 Jan. – 13 Feb.
90 2014. Data referenced in this paper are primarily from a proton-transfer-reaction mass-
91 spectrometer (PTR-MS), deployed in both 2012 and 2013, and a gas chromatograph with flame
92 ionization detection (GC-FID), deployed in 2013. Measurements from 2014 are not discussed in
93 this analysis.

94
95 PTR-MS uses chemical ionization with H_3O^+ ions to selectively detect VOCs (de Gouw and
96 Warneke, 2007). The technique is particularly sensitive to aromatic and small oxygenated VOCs,
97 but cannot detect small alkanes due to their low proton affinity. The instrument deployed at Horse
98 Pool uses a quadrupole mass filter with unit mass resolution that scans through a set of selected
99 ions every 38 seconds. Data are averaged to a 1-minute time scale. Calibrated measurement
100 accuracy is generally better than 20%, with a precision of 10%. The instrument is not able to
101 distinguish between isomers; e.g. a measurement of C8 aromatics comprises the sum of
102 ethylbenzene, o-, m-, and p- xylenes. Comparison with a high-resolution PTR- time-of-flight
103 spectrometer operated by the University of Wyoming (Warneke et al., 2015) indicates negligible
104 contribution from isobaric compounds (e.g., benzaldehyde).

105
106 The GC-FID deployed at Horse Pool resolves C2-C7 saturated and unsaturated hydrocarbons.
107 Ambient air passes through water and carbon dioxide traps, then into a liquid nitrogen cryogenic
108 VOC trap. VOCs are captured in the cryogenic trap for five minutes every half hour. After the
109 five-minute sampling period, compounds are injected onto a 50m $\text{Al}_2\text{O}_3/\text{KCl}$ PLOT column and
110 analyzed using flame ionization detection. The accuracy and precision are dependent on compound
111 and sample flow rate, but are generally <20% and <5%, respectively. The instrument has been
112 previously described in more detail by Kuster *et al.* (2004).

113
114 Other measurements used in this paper include gas-chromatography mass-spectrometry (GC-MS)
115 operated in 2012 (Gilman et al., 2010), methane cavity ring-down spectroscopy (CaRDS, Picarro)
116 operated in 2013 (Crosson, 2008), organic aerosol via quartz filter collection/thermal desorption
117 in 2013 (Bates et al., 2004), snow organic carbon using a Shimadzu TOC-VCSH instrument in
118 2013, and organic peroxy nitrate (PAN) species by chemical ionization mass spectrometry (Slusher
119 et al., 2004). Some sulfur-containing species were measured (Li et al., 2014) but are not discussed
120 in this manuscript. Further details on sampling methods and conditions, meteorological
121 measurements, and calibrations are described in a summary report (Uinta Basin: 2013 Winter
122 Ozone Study: Final Report; available at
123 <http://www.deq.utah.gov/locations/U/uintahbasin/ozone/strategies/studies/UBOS-2013.htm>).

124

125 2.2 Data treatment

126 A stagnation event associated with high levels of ozone formation occurred from 29 Jan. to 10
127 Feb. 2013. A subset of this period, 31 Jan. 2013 20:48 (LT) through 08 Feb. 2013 05:29, is
128 analyzed here (Fig. 1). This period captures the majority of the ozone formation event, is
129 characterized by a strong temperature inversion, and avoids periods of higher wind on 31 Jan. and
130 08 Feb. Selecting these meteorological conditions minimizes changes in VOC concentrations and
131 ratios due to mixing into or out of the basin.

132
133 Primary hydrocarbons and oxygenated compounds investigated are listed in Table 1. The majority
134 of analysis was applied to compounds measured by PTR-MS. The fast time resolution of this
135 instrument (1 minute) allows the separation of plumes of VOCs from nearby sources from the
136 more regionally widespread, accumulated emissions in the basin. Additionally, restricting
137 analyzed compounds to a single instrument helps eliminate instrumental variation. ~~C6-C10~~
138 ~~aromatic VOCs were selected for analysis because they have readily identifiable parent masses,~~
139 ~~they are sensitively detected by PTR-MS, and have a relatively wide range of reactivity with OH~~
140 ~~($k_{OH} = 1.22 \times 10^{-12} \text{ s}^{-1}$ to $56 \times 10^{-12} \text{ s}^{-1}$).~~ Additional compounds from the GC-FID data set were used
141 to investigate the balance of primary and secondary species.

142
143 Concentrations of VOCs during an inversion event displayed rapid, diurnal, and multi-day
144 variability (Fig. 2). Some of this variability is attributable to meteorology (such as changes in
145 boundary layer height during the day, or temporary shifts in wind direction bringing pollution from
146 nearby sources), and some to chemistry, but the relative contributions can be difficult to separate.
147 Analysis of ratios of VOCs provides a way to isolate the effects of chemistry from meteorology.
148 This is a common and flexible approach: applications have included determining the
149 photochemical age of urban emissions (Roberts et al., 1984; de Gouw et al., 2005), quantifying
150 halogen chemistry in arctic air (Jobson et al., 1994), and identifying contributions from oil and
151 natural gas operations to ambient pollution (Gilman et al., 2013).

152
153 Measurements of primary compounds by PTR-MS showed frequent 1-3 minute duration episodes
154 with very high mixing ratios, at least 50% higher than short-term average concentration. These
155 spikes signify interception of plumes of un-aged emissions and are not representative of the bulk

156 air composition at the Horse Pool site. An hourly running median was applied to separate longer-
 157 term variability from transitory primary emissions (Fig. 2). For consistency, an hourly running
 158 median was also applied to oxygenated compounds. The ratio of each VOC to benzene was then
 159 determined. Benzene is a well-calibrated compound with few interferences on the PTR-MS;
 160 additionally, good agreement with other instrumentation (GC-FID and PTR-ToF) at the site affords
 161 a high level of confidence in this measurement (Warneke et al., 2015).

162

163 3. Results and Discussion

164 3.1 Primary compounds

165 Primary compounds are defined as those species that are directly emitted and not formed by
 166 photochemistry. The rate of change with time of a single, primary VOC can be written as

$$167 \frac{d[VOC]}{dt} = P_{VOC} - k_{VOC}[OH][VOC] - \sum D_i[VOC] \quad (1)$$

168 where P_{VOC} is the emission rate of the VOC and k_{VOC} is the rate constant for the reaction of the
 169 VOC with OH. P_{VOC} is a volumetric input with units of molecule $\text{cm}^{-3} \text{s}^{-1}$ and describes how direct
 170 emission increases observed VOC concentrations. The only chemical loss term included is reaction
 171 with OH, the major oxidizing radical in this environment. Previous modeling has suggested that
 172 VOC reactions with other radicals, such as Cl^\bullet , were negligible in comparison to reaction with OH
 173 (Edwards et al., 2014). Additionally, reaction rates of the primary species considered here (C6-
 174 C10 aromatics) with O_3 and NO_3 are at least several orders of magnitude lower than reaction rates
 175 with OH (Atkinson and Arey, 2003). D_i are rate constants for first-order loss processes; e.g.
 176 deposition, dilution, photolysis, etc. If two VOCs, “A” and “B”, behave according to Equation (1),
 177 we can derive the rate of change of their ratio ($[A]/[B]$) as follows:

$$178 \text{ratio}(t) = \frac{[A](t)}{[B](t)} \quad (2a)$$

179 Using the partial derivatives of $\text{ratio}(t)$ with respect to $[A]$ and $[B]$, the rate of change of the ratio
 180 is:

$$181 \frac{d(\text{ratio})}{dt} = \frac{1}{[B]} \frac{d[A]}{dt} - \frac{[A]}{[B]^2} \frac{d[B]}{dt} \quad (2b)$$

182 Then, substituting Equation (1) for dA/dt and dB/dt , we arrive at:

$$183 \frac{d(\text{ratio})}{dt} = \frac{P_B}{[B]} (ER - \text{ratio}) + (\text{ratio})[OH](k_B - k_A) + \sum (\text{ratio})(D_{iB} - D_{iA}) \quad (2c)$$

184

185 The primary emission rate (P_B), emission ratio (ER), and the concentration of OH are unknown.
186 The emission ratio ($ER=P_A/P_B$) is the ratio of two VOCs in fresh emissions (time $t = 0$) and is a
187 measure of source composition. We consistently used benzene as the denominator in the ratio, so
188 that $[B] = [\text{benzene}]$, P_B is the emission rate of benzene, ER is the emission ratio of a VOC to
189 benzene, and so on. Meteorological data and the measured ambient mixing ratio of benzene were
190 used to determine the number density of benzene ($[B]$) as a function of time. These values were
191 referenced directly when applying Equation (2c).

192
193 C6-C10 aromatic VOCs were selected for analysis because they have readily identifiable parent
194 masses, they are sensitively detected by PTR-MS, and have a relatively wide range of reactivity
195 with OH ($k_{OH} = 1.22 \times 10^{-12} \text{ s}^{-1}$ to $56 \times 10^{-12} \text{ s}^{-1}$). Application of this analysis to VOCs measured by
196 PTR-MS using Equation (2c) includes the following assumptions.

197
198 (1) For each first-order loss process, rate constants are nearly identical for aromatic compounds
199 ($D_{iA}=D_{iB}=D_i$). These loss processes include mixing out of the basin, photolysis, and deposition.
200 Mixing is dependent on dynamics and not on chemical characteristics, so mixing loss rate constants
201 should be identical for all VOCs with the same vertical concentration profile ($D_{mixing,B} -$
202 $D_{mixing,A} = 0$). We saw no evidence of differences in vertical gradients of aromatic species at
203 Horse Pool. As concentrations of VOCs in the background atmosphere were considerably smaller
204 than VOC concentrations inside the basin, changes in VOC ratios due to mixing in of background
205 air are negligible. Integrated UV absorption cross-sections of C6-C10 aromatic hydrocarbons are
206 small and similar to one another (Etzkorn et al., 1999), so ($D_{photolysis,B} - D_{photolysis,A}$) is likely
207 negligible compared to primary emission and reaction with OH. The same argument can be made
208 for wet or dry deposition ($D_{deposition,B} - D_{deposition,A} \cong 0$), as monocyclic aromatic compounds
209 are structurally similar and have small solubilities in water. The terms ($D_{iB} - D_{iA}$) can therefore
210 be eliminated.

211
212 (2) Primary VOC emission rate and emission ratios are constant in time and similar in composition
213 across the basin – we cannot confidently parameterize a more complicated emissions scenario with
214 available data, nor is there any evidence supporting or reason to assume a change in emissions
215 with time of day.

216

217 (3) Finally, on an hourly scale, we assume that compounds are well mixed. The latter assumptions
218 are supported by aircraft measurements in Jan-Feb. 2013, which found elevated VOC
219 concentrations with similar ratios in all parts of the basin, including regions with varying intensities
220 and types of fossil fuel extraction activity (Oltmans et al., 2014). The time period analyzed,
221 characterized by a strong temperature inversion and light winds (Fig. 1), was specifically selected
222 to support these assumptions.

223

224 **3.1.1 Emission rates and ratios**

225 The analysis is first applied to night-time data only (any points where solar radiation is zero), to
226 estimate P_B and ER . During the night, OH is close to zero and Eq. (2c) reduces to

$$227 \quad \frac{d(\text{ratio})}{dt} = \frac{P_B}{[B]} (ER - \text{ratio}) \quad (3)$$

228 This method, using only night-time data, reduces the number of free variables. It completely
229 separates primary emission from OH chemistry. Additionally, it allows the use of C9 and C10
230 aromatics measurements, as the OH rate constants for these groups are not well constrained.

231

232 The measured ratios of C7, C8, C9, and C10 aromatics to benzene were described using a best fit
233 of Eq. (3) to the data. The free parameters in this fit are P_B and ER . A best fit was determined
234 separately for each of the four aromatic ratios, providing four, similar, independent estimates of
235 P_B (Fig. 3) and four emission ratios to benzene (Table 2). We evaluate the fit by comparing
236 emission ratios to literature values and the composition of plumes from nearby sources, and,
237 second, by comparing emission rate to an independent estimate.

238

239 The derived emission ratios from this analysis represent an averaged source composition of all
240 point sources contributing VOCs to well-mixed air. In Fig. 4, the derived emission ratios are
241 compared to three other measurements of source composition in the Uintah basin: (1) Mobile
242 laboratory measurements taken at individual wellpads in 2012 (Warneke et al., 2014); (2) ambient
243 measurements taken at Horsepool in 2012 (Warneke et al., 2014); and (3) 2013 VOC enhancement
244 ratios in spikes above a 1-hour running median (discussed above). These spikes are likely plumes
245 of fresh emissions from nearby wellpads. The fastest-reacting C10 aromatic (1,2,4-
246 trimethylbenzene) had a peak daytime chemical lifetime against OH of about 30min. Seven other

247 wellpads were within 500m of the Horsepool site; given average wind speed (1.6 m s^{-1}), this
248 corresponds to a 5 minute transport time – much shorter than the chemical lifetime of any of the
249 analyzed aromatic species. All three measurements are separated into gas-producing and oil-
250 producing well contributions; in mobile lab data, by type of wellpad sampled; in Horsepool data,
251 by correlation with wind direction (Warneke et al., 2014).

252
253 There is a clear distinction between oil and gas sources. The difference grows with carbon number;
254 i.e. gas producing-wells emit a lighter mixture of VOCs. Emission ratios suggested by our analysis
255 suggest significant contribution from both oil and gas sources. In addition to the oil/gas distinction,
256 there is a large range of variability in source composition of aromatic species. This variability is
257 difficult to represent in bulk emissions estimates and models. Together with supporting evidence
258 from aircraft that emissions were reasonably well mixed across the basin (Oltmans et al., 2014),
259 our analysis provides an independent measure of average emissions composition.

260
261 The average benzene emission rate was $4.1 \pm 0.4 \times 10^5$ molecules $\text{cm}^{-3} \text{ s}^{-1}$. To evaluate this emission
262 rate estimate, we compare to basin-wide methane emission measurements conducted by aircraft in
263 2012 (Karion et al., 2013). To our knowledge this is the only recent top-down emissions estimate
264 for the Uintah Basin. Karion et al. determined that basin-wide methane emissions were $55 \pm 15 \times$
265 10^3 kg hr^{-1} . To compare a volume-normalized estimate (molecules benzene $\text{cm}^{-3} \text{ s}^{-1}$) to the whole-
266 basin estimate ($\text{kg methane hr}^{-1}$), we need (1) the emission ratio of methane to benzene and (2) the
267 total volume of the polluted layer during the 2013 ozone episode.

268
269 A strong correlation between methane and benzene is apparent from ground site measurements at
270 Horse Pool in 2012 and 2013 (Fig. 5). Aircraft flask samples taken in 2013 suggest that the
271 methane:benzene ratio is independent of location in the basin – it was similar in both the eastern
272 gas field and western oil field (Oltmans et al., 2014). The methane:benzene emission ratio was
273 approximated from 2012 measurements and 2013 plumes ($\text{ER} = 1330 \pm 80 \text{ ppbv/ppbv}$).

274
275 The polluted volume of the basin was determined from frequent ozonesonde measurements at a
276 number of locations in the basin, as well as aircraft profiles. They showed well mixed ozone
277 concentrations up 1600-1700 meters above sea level (100-200 meter above ground level at

278 Horsepool), above which mixing ratios decreased sharply (Oltmans et al., 2014). Taking the terrain
279 of the basin into account, we then integrate the volume of the basin from the surface to the mixing
280 height. The uncertainty in the basin wide methane emission estimate is dominated by the
281 uncertainty in this volume, and we report the values determined from minimum and maximum
282 polluted layer altitude (1600m – 1700m).

283
284 Using the methane:benzene ratio and the mixing volume of the basin, we derive an emission rate
285 of $(14-39) \times 10^3$ kg methane hr^{-1} . This is lower than the Karion et al. estimate, but of the same
286 magnitude. An inspection of well locations in the basin shows that a significant fraction (40-50%)
287 of wells lie outside the polluted layer (Fig. 6). An aircraft flux measurement would have likely
288 included contributions from these wells, whereas our analysis only included wells emitting inside
289 the isolated polluted volume. A linear extrapolation based on the number of wells inside and
290 outside the polluted volume suggests an emission rate of $(27-57) \times 10^3$ kg methane hr^{-1} , which
291 overlaps with the Karion et al. value. Although this estimate is considerably less precise than the
292 aircraft flux measurement, it does confirm that the best-fit values of benzene emission rate are
293 plausible.

294 **3.1.2 Concentration of OH radical**

295 The full time series (both day and night) was analyzed over the buildup period, using Eq. (2c). The
296 primary emission term (P_B) and the emission ratio were fixed as determined from the night best
297 fits. The only remaining free variable is the concentration of OH.

298
299 The calculation requires OH rate constant (k_{OH}) for the aromatics. Measurements of C8 aromatics
300 in 2013 were not isomerically resolved by PTR-MS and represent the sum of ethylbenzene and *o*-
301 , *m*-, and *p*-xylenes. Speciated measurements of C8 aromatics by GC-MS were made in 2012,
302 when photochemical aging of VOCs was less active and the bulk air composition more closely
303 resembled primary emissions. The 2012 GC-MS measurements were used to compute a weighted
304 average OH rate constant for the C8 aromatics group. The OH rate constants for individual species
305 in this group are within a factor of 2.1 of the mean. The groups C9 and C10 aromatics contain a
306 much larger number of isomers, with a wider variance in OH rate constants. Not all these isomers
307 were measured by GC-MS in 2012, and some of the OH rate constants are unknown. Therefore,
308 the group average rate constant could not be constrained in the same way.

309
310 To parameterize the diurnal variation in OH, we constrained OH to be proportional to solar actinic
311 flux. It is well established that [OH] is strongly linearly correlated with UV light intensity (Hard
312 et al., 1986; Rohrer and Berresheim, 2006). A best fit and an average value of OH was computed
313 separately for both toluene and C8 aromatics according to Eq. (3) (shown in Fig. 3). Results are
314 included in Table 2. The average of these two values was used as the concentration of OH in further
315 analysis.

316
317 Using this [OH], the k_{OH} for C9 and C10 aromatics were allowed to vary. Best fits for the C9 and
318 C10 aromatics were calculated and are shown in Fig. 3. The group average rate constants (Table
319 2) are within the range of values known for isomers of C9 and C10 aromatics. For C9 aromatics,
320 the group average rate constant was determined to be $16.9 \text{ cm}^3 \text{ molecule}^{-1} \text{ s}^{-1}$; known values range
321 from 5.3 (n-propylbenzene) to $56.7 \text{ cm}^3 \text{ molecule}^{-1} \text{ s}^{-1}$ (1,3,5-trimethylbenzene) (Atkinson and
322 Arey, 2003). For C10 aromatics, the group average rate constant was determined to be 24.2 cm^3
323 $\text{molecule}^{-1} \text{ s}^{-1}$; known values range from 4.5 (t-butylbenzene) (Atkinson and Arey, 2003) to 55.5
324 $\text{cm}^3 \text{ molecule}^{-1} \text{ s}^{-1}$ (1,2,4,5-tetramethylbenzene) (Aschmann et al., 2013). The average rate constant
325 constrains group composition, and could be useful in future investigations of photochemical
326 processing.

327
328 Knowledge of typical daily OH concentrations is crucial to understand photochemical processing
329 of VOCs and ozone production. OH was not measured directly in 2013, but our analysis provides
330 an estimate of OH exposure that is constrained by solar actinic flux and VOC measurements. OH
331 peaked daily at $1 \times 10^6 (\pm 21\%) \text{ molecule cm}^{-3}$, which is low compared to urban areas affected by
332 photochemical smog with typical OH concentrations between $(5-10) \times 10^6 \text{ molecule cm}^{-3}$ (Shirley
333 et al., 2006). We compare to an independent estimate of [OH] in 2013 using the Master Chemical
334 Mechanism v.3.2 (MCM) framework (Edwards et al., 2014). The MCM OH estimate is generated
335 using more than 12000 explicit reactions comprising degradation schemes for nearly all
336 hydrocarbons measured at the Horse Pool site and has been applied previously to photochemistry
337 in the Uintah Basin (Edwards et al., 2014; Edwards et al., 2013). The agreement between our
338 model and the MCM estimate in peak daytime concentration is within a factor of 1.7 overall and
339 differs by only 2% on 5 Feb. 2013 (Fig. 7). The agreement is especially good considering that OH

340 values in our analysis are constrained by measured photolysis rates and a single scaling factor, and
341 so cannot generate the multi-day trend seen in the MCM calculation. This excellent agreement
342 substantiates the chemistry described by the MCM model.

343

344 3.2 Oxygenated compounds

345 Oxygenated compounds may also have photochemical sources. For these species, the change in
346 concentration with time is controlled by the production rate via photochemistry, loss to reaction
347 with OH, and first-order loss processes such as mixing, photolysis and deposition. The rate of
348 change can be written similarly to Eq. (1):

$$349 \frac{d[VOC]}{dt} = Yield * k_{precursors}[OH][precursors] - k_{VOC}[OH][VOC] - D[VOC] \quad (4)$$

350 Here [precursors] is the sum concentration of all precursor species, *Yield* is the fraction of reactions
351 with OH that form the product compound, and $k_{precursors}$ is the weighted average OH rate constant
352 of precursor species. Again, *D* represents first-order loss processes. The oxygenated species
353 considered here are ~~formaldehyde, acetaldehyde, acetone, 2-butanone (MEK), formic acid, and~~
354 ~~methanol, and formaldehyde.~~

355

356 As with Eq. (2c), the rate of change of the ratio of a photochemically produced compound to
357 benzene is:

$$358 \frac{d(ratio)}{dt} = Yield * k_{precursors}[OH] * R_{PB} - (ratio) * \left([OH](k_{prod} - k_B) + J + \frac{P_B}{[B]} \right) \quad (5a)$$

$$359 = \lambda_f * [OH] - (ratio) * \left([OH](k_{prod} - k_B) + J + \frac{P_B}{[B]} \right) \quad (5b)$$

360 R_{PB} is the ambient ratio of precursor species to benzene, k_{prod} and k_B are the OH rate constants of
361 the product species and benzene, and *J* is the photolysis rate constant of the product species. Here
362 we again assume that other first-order processes, mixing and deposition, are not significantly
363 different between the oxygenated VOCs and benzene. ~~We also assume that the only source of these~~
364 ~~species is photochemistry; i.e. they are not emitted directly from primary sources. Primary~~
365 ~~emission of methanol and formaldehyde is considered separately later in the analysis (below).~~ On
366 the other hand, most of these compounds contain a carbonyl functional group, and photolysis rates
367 could be significant. *J* was set proportional to solar actinic flux and scaled to photolysis constants
368 from the literature (values and literature sources are given in Table 3). We also assume that the
369 only source of these species is photochemistry; i.e. they are not emitted directly from primary

370 sources. Methanol and formaldehyde are included in this section as they are oxygenated species.
371 However, the high observed mixing ratios of methanol and formaldehyde (Table 1), previous
372 modeling work (Edwards et al., 2014), and knowledge of industry practices indicates that these
373 two species also have direct (primary) sources. We first analyzed methanol and formaldehyde
374 assuming solely photochemical sources, to investigate the extent to which secondary formation
375 can explain their behavior. We then modified the analysis to consider primary emission of these
376 species. Methanol and formaldehyde are discussed separately in the analysis (below).

377
378
379 As the relative amounts of precursor species and their product yields were unknown, *yield*,
380 $k_{precursors}$, and R_{PB} were bundled into a single free variable, λ_f (formation rate constant). The term
381 R_{PB} requires further discussion. The analysis of primary compounds (above) shows that the ratios
382 of C7-C10 aromatics to benzene are highly variable and depend on photochemical exposure. R_{PB} ,
383 the ratio of precursor species to benzene, should also change over time. However, in applying
384 Equation (5b), we have simplified analysis by treating R_{PB} as approximately constant. By volume,
385 the dominant VOCs measured at Horse Pool were C1-C5 alkanes. These compounds react more
386 slowly with OH than C7-C10 aromatics. Reaction with OH has a proportionally smaller effect on
387 their concentrations, and indeed, ratios of these compounds to benzene show less diurnal
388 variability (Fig. 8a). Despite how slowly these compounds react with OH, the very large
389 concentration of these compounds means that they C2-C5 alkanes account for most of the reactions
390 between OH and VOCs, and are the most important precursor compounds (Fig. 8b). We can
391 therefore use the simplifying approximation of constant precursor:benzene ratio.

392
393 Again, the analysis was first applied to night data only. During the night, (5b) reduces to:

$$394 \frac{d(\text{ratio})}{dt} = -(\text{ratio}) \left(\frac{P_B}{[B]} \right) \quad (6)$$

395 Using Equation (6), a best fit was calculated for acetaldehyde, formic acid, acetone, MEK,
396 methanol, and formaldehyde (Fig. 9), providing six values of the primary benzene emission rate
397 (P_B) (Table 3).

398
399 The best fit functions to acetone, acetaldehyde, formic acid, and MEK for nighttime data only were
400 able to predict a decreasing trend in the ratio of VOC:benzene, but did not replicate the strong

401 decrease in ratio towards the end of the night. Primary emission of benzene during the night could
402 only account for a portion of the decrease, signifying an additional oxygenate removal process not
403 included in Equation (6). A possible candidate is increased deposition of oxygenates. Including a
404 free first-order deposition variable did not significantly affect model output, suggesting a complex
405 process increasing in strength during the night. One possibility is deposition on ice crystals.
406 Surfaces, including the sampling inlet, typically gained a thick coating of ice rime during the night,
407 creating additional surface area available for deposition. This process would also affect polar
408 oxygenated species much more than primary hydrocarbons, consistent with the additional decrease
409 in oxygenates not observed with aromatics. Because this process affected our sampling inlet, it is
410 possible that oxygenate behavior during early morning is an inlet artifact rather than a significant
411 basin-wide process. We removed rime ice from the sampling inlet early each morning, and other
412 surfaces were typically free of rime by mid-morning (snow cover remained during the day).

413

414 The values of benzene emission rate derived from night-only best fit to acetone, acetaldehyde,
415 formic acid, and MEK were slightly higher than estimates from primary compounds: 5×10^5 as
416 opposed to 4×10^5 molecule $\text{cm}^{-3} \text{s}^{-1}$. This is consistent with an undetermined additional removal
417 process. In the absence of an appropriate loss term, a best fit using Equation (6) would artificially
418 increase the benzene emission rate to reproduce the stronger downwards trend in ratio.

419

420 The diurnal behaviors of methanol and formaldehyde differ significantly from other species. The
421 ratios of methanol and formaldehyde to benzene do not increase steadily during the day and do not
422 decrease at night. Additionally, the values of primary benzene emission rate determined from
423 methanol and formaldehyde are at least a factor of two smaller than values determined from any
424 other compound. ~~For methanol, this behavior is almost certainly due to large primary sources. A~~
425 ~~plausible explanation for this behavior is primary emission of these two compounds.~~ Methanol is
426 used by the oil and natural gas industry in a variety of applications in the basin (Lyman, 2014),
427 including storage of methanol containers on wellpads, and direct emissions of methanol associated
428 with this use are very high as witnessed by hourly average mixing ratios in the basin, which can
429 build up to more than 200 ppbv. It is therefore unsurprising that methanol variation is poorly
430 described by Equation (6). Primary sources of formaldehyde are less clear. Incomplete combustion
431 and emission from dehydrators, separators, compressors, flares, oil pumps and processing plants

432 have been suggested as sources, but are not well quantified in the Uintah basin. Additionally, there
433 is no easily distinguishable correlation between formaldehyde and NO_x, so it is not clear that
434 combustion is a significant source of formaldehyde. In accordance with our findings, Edwards et
435 al. (2014) left the option open for primary emissions of formaldehyde due to the inability of the
436 MCM model to reproduce the ambient mixing ratios.

437
438 To investigate primary emission of methanol and formaldehyde we modified Equation (6) in
439 several ways. First, we added a term representing primary emission of oxygenates and determined
440 best-fit values of benzene emission rate and oxygenate:benzene emission ratio. χ^2 values decreased
441 insignificantly (-5%, methanol) and slightly (-22%, formaldehyde) and calculated values of
442 primary benzene emission rate were unreasonable (8×10^5 and 1×10^6 molecules $\text{cm}^{-3} \text{s}^{-1}$ from the
443 methanol and formaldehyde analysis, respectively). Next, we fixed the primary benzene emission
444 rate to the value determined from the primary compounds analysis and determined emission ratios
445 for methanol and formaldehyde only. Emission ratios of formaldehyde:benzene and
446 methanol:benzene were 1.01 and 10.3. These values are slightly less than the ambient ratios,
447 consistent with accumulation from both photochemistry and primary emission. However, the best
448 fit still did not capture the majority of measurement variability and may not be accurately
449 characterizing physical processes affecting methanol or formaldehyde. For instance, an emission
450 source poorly correlated with benzene would not be well represented by Equation (6).

451
452 Because of possible complex deposition of oxygenated species during the night, and primary
453 emission of methanol and formaldehyde, emission rates derived from the analysis of these
454 oxygenates are less likely to be accurate than those derived from analysis of primary species. We
455 elected to exclude night data from further analysis, and retain the primary benzene emission rate
456 (P_B) determined from the primary compounds model. The fit of Equation (5b) was then calculated
457 for acetone, MEK, acetaldehyde, and formic acid, using daytime data (Fig. 9), to determine values
458 of the formation rate constant (λ_f) for each compound (Table 3).

459
460 The best-fit of daytime oxygenate ratios is better able to explain the measurements, with R^2 values
461 of 0.4 to 0.8 (Table 3). Values of the formation rate constant (λ_f) are plausible. For instance, the
462 best-fit value of λ_f for acetone is $8.72 \times 10^{-11} \text{ cm}^3 \text{ molecule}^{-1} \text{ s}^{-1}$. The main precursors of acetone

463 present in the Uintah Basin were iso-butane and propane. The weighted average rate constant for
464 reaction of iso-butane and propane with OH is $1.3 \times 10^{-12} \text{ cm}^3 \text{ molecule}^{-1} \text{ s}^{-1}$ and the mol ratio of
465 these compounds to benzene was approximately 70. Assuming that all propane-OH and iso-
466 butane-OH reactions formed acetone, the calculated λ_f for acetone is $9.1 \times 10^{-11} \text{ cm}^3 \text{ molecule}^{-1} \text{ s}^{-1}$,
467 which is very close to the best-fit calculated value. The high R^2 values and reasonable λ_f suggest
468 that Equation (5b) captures the most important daytime processes affecting acetone, acetaldehyde,
469 MEK, and formic acid.

470

471 **4. Organic carbon budget**

472 In this section, we categorize VOCs as either primary (directly emitted) or secondary (enhanced by
473 oxidative chemistry), and quantify the total organic carbon mass in each category. Using two
474 complementary mass balance approaches, we show that one would expect to see more oxygenated species
475 than were measured. Both approaches rely on conservation of organic carbon mass: when a primary
476 compound is oxidized, the total mass of organic carbon does not change. This is true regardless if
477 the molecule's structure changes, if it fragments into several smaller molecules, if subsequent
478 reactions form higher generation products, or if it moves into a different reservoir (e.g. aerosol or
479 snowpack).

480

481 First, carbon mass concentration is conserved. The total organic carbon mass of primary compounds
482 lost to oxidation must be equal to the total organic carbon mass gained by secondary compounds.
483 To quantify this mass, we use the loss rate of a primary compound to oxidation:

$$484 \left. \frac{d(\text{primary VOC})}{dt} \right|_{\text{chemical}} = -k_{\text{PrimaryVOC}}[\text{OH}][\text{primary VOC}] \quad (7)$$

485 The amount of organic carbon lost from all primary species measured by PTR-MS and GC-FID
486 (compounds listed in Table 1) during the stagnation event can be found by integrating Equation
487 (7) for each individual primary VOC, then summing the results over all primary VOCs. For
488 completeness, methane (from CaRDS) was also included. [OH] was set to the values calculated
489 above (Table 2). OH rate constants for C8, C9, and C10 aromatics were taken from Table 2, and
490 OH rate constants for all other species were taken from Atkinson and Arey, 2003.

491

492 Because total carbon mass is conserved, the total carbon mass lost from primary species is equal
493 to the total carbon mass gained by all secondary species. This value, about $3.7 \times 10^{-10} \text{ gram C cm}^{-3}$

494 on day 6 of the stagnation event, is the calculated or expected mass of secondary species. Measured
495 oxygenates and secondary species, including methanol, formaldehyde, formic acid, acetone,
496 acetaldehyde, MEK, PAN species (peroxyacrylic nitric anhydride (APAN), peroxyacrylic
497 nitric anhydride (MPAN), peroxyacetic nitric anhydride (PAN), and peroxypropionic nitric
498 anhydride (PPN)), organic carbon in snow, and PM2.5 organic aerosol, only sum to 0.64×10^{-10}
499 gram C cm⁻³, or 17% of calculated secondary carbon mass.

500
501 Methanol and formaldehyde have substantial primary sources, so including them in this calculation
502 artificially increases the percentage of secondary species accounted for: 0.64×10^{-10} gram C cm⁻³ is
503 an upper bound to the mass of measured secondary species. If we assume methanol is entirely
504 primary, measured secondary species only sum to 0.48×10^{-10} gram C cm⁻³, or 12.9% of calculated
505 secondary carbon mass. If we assume both methanol and formaldehyde have no photochemical
506 sources, measured secondary species sum to 0.46×10^{-10} gram C cm⁻³, or 12.5% of calculated
507 secondary carbon mass. Figure 10 shows the upper bound to measured secondary species
508 (including both methanol and formaldehyde).

509
510 This gap between the calculated (expected) mass of secondary species and the measured mass of
511 secondary species is a factor of 5.8 (Fig. 10). Other measurement and modeling studies of the
512 Uintah Basin suggest that unquantified secondary species are responsible for a large part of this
513 gap: many additional oxygenated VOCs were detected, but not quantified, by PTR-time-of-flight
514 (PTR-ToF) mass spectrometry (Warneke et al., 2015), and MCM modeling indicates that carbonyl
515 groups formed from higher-weight species (e.g. aromatics) were not only abundant but major
516 drivers of ozone formation.

517
518 Oxidation of quantified secondary species to CO and CO₂, or loss to mixing out of the basin are
519 alternate explanations that could account for some of the disparity. Using a second carbon mass
520 balance technique, we show that unquantified secondary species are an important factor. The
521 second technique compares oxidation rates: the oxidation loss rate of primary species must be
522 equal to the photochemical formation rate of secondary species. Neither of these processes is
523 affected by higher-generation oxidation reactions or loss to mixing or deposition. A disparity
524 between the carbon mass loss rate to oxidation of primary species and the formation rate of

525 measured secondary species means that there must be other, unquantified, secondary species
526 forming. Therefore, comparing oxidation and formation rates provides a way to determine if the
527 mass disparity between calculated and measured secondary species is at least partly due to
528 unquantified compounds.

529
530 The total oxidation rate of primary species was determined by applying Equation (7) to each
531 measured primary species, then summing over all primary species. The formation rate of quantified
532 secondary species was determined using Equation (4). The first term in Equation (4),
533 $Yield * k_{precursors}[OH][precursors]$, is the formation rate of a secondary VOC. To clarify, this
534 is the rate at which a secondary VOC is produced by oxidation chemistry, not the rate of net
535 increase in mass (net = formation – loss). As in Equation (5b), this can be simplified to

$$536 \left. \frac{d(\text{secondary VOC})}{dt} \right|_{\text{formation}} = \lambda_f [OH][benzene] \quad (8a)$$

$$537 \lambda_f = Yield * k_{precursors} * \frac{[precursors]}{[benzene]} \quad (8b)$$

538 λ_f is the formation rate constant, and was (above) determined for acetone, acetaldehyde, formic
539 acid, and MEK. The oxidation rate of primary compounds is a factor of two higher than the
540 formation rate of acetaldehyde, acetone, formic acid, and MEK (Fig. 11). This large disparity
541 indicates a substantial presence of unquantified secondary species. The formation rate of these
542 species is $3.2(\pm 1.2) \times 10^{-16}$ g C cm⁻³ s⁻¹ on average or 60(±23) ppbv C day⁻¹.

543

544 5. Conclusions

545 High concentrations of organic carbon species (up to 5 ppm nonmethane carbon) associated with
546 oil and natural gas extraction were measured at a rural site in the Uintah Basin, Utah, during the
547 winter of 2013. A relatively simple analysis was applied to measurements of aromatic species by
548 PTRMS to explain variation in their ratios due to reaction with OH and primary emission. The
549 analysis was extended to measurements of small oxygenated compounds by PTRMS, with the goal
550 of explaining ratios of these compounds to benzene in terms of production and loss via OH
551 chemistry, photolysis, and primary emission. Results of both analyses were used to develop a
552 carbon mass budget, to determine the relative fractions of carbon in primary and secondary species.

553

554 The analysis of primary aromatic species provided plausible estimates of [OH], aromatic VOC
555 emission ratios, and benzene emission rate. The daily peak of [OH] was low (1×10^6 molecule cm^{-3}),
556 consistent with MCM modeling and highlighting the unusual oxidation chemistry occurring in
557 this region. Emission ratios indicate source contributions from both oil and gas wells. Using
558 measured correlation between benzene and methane, the benzene emission rate ($4.1 \pm 0.4 \times 10^5$
559 molecule $\text{cm}^{-3} \text{ s}^{-1}$) was extrapolated to a basin-wide methane emission rate ($27\text{-}57 \times 10^3$ kg methane
560 hr^{-1}) in order to compare with an independent top-down estimate from aircraft. Although the large
561 uncertainties associated with the extrapolation of the benzene emission rate to a basin-wide
562 methane emission rate preclude the use of our estimate as an assessment of regulatory inventories,
563 the agreement with the 2012 aircraft methane flux value supports the plausibility of our analysis.
564 Our analysis was not able to completely explain night time variability of small oxygenated VOCs,
565 whose behavior may be affected by primary emission (methanol and formaldehyde) and deposition
566 to ice surfaces. However, a best fit to day time data provided values of carbonyl formation rate
567 consistent with expected formation rates from known precursors. The calculated carbon budget
568 indicated that a large fraction of secondary carbon mass (83%, or 3×10^{-10} gC cm^{-3}) is unaccounted
569 for. A comparison of measured carbonyl formation rates to primary compound oxidation rates
570 indicated substantial presence of unquantified secondary species.

571
572 The analysis method outlined here is relatively simple, including just a few terms for basic
573 chemistry and primary emission. It uses little computer processing power and references only
574 measurements that can be made with standard VOC instrumentation. Despite its simplicity, this
575 method is able to provide considerable information on VOC chemistry, including source
576 composition and emission rates, the concentration of OH, and measurement thoroughness. Best-
577 fit values are very reasonable and support findings from more complicated chemical models. A
578 similar analysis could be applied to investigations of other regions where VOC pollutants are
579 geographically or meteorologically contained, especially where detailed chemical measurements
580 are unavailable or not possible.

581
582 *Acknowledgements.* The Uintah Basin Winter Ozone Studies were a joint project led and
583 coordinated by the Utah Department of Environmental Quality (UDEQ) and supported by the
584 Uintah Impact Mitigation Special Service District (UIMSSD), the Bureau of Land Management

585 (BLM), the Environmental Protection Agency (EPA), and Utah State University. This work was
586 funded in part by the Western Energy Alliance, and NOAA's Atmospheric Chemistry, Climate,
587 and Carbon Cycle Program. We thank Questar Energy Products for site preparation and support.
588 We thank Colm Sweeney (NOAA GMD) for the use of a Picarro methane instrument, and Shane
589 Murphy and Jeffrey Soltis (University of Wyoming) for the use of a Picarro methane instrument.
590 We thank NOAA Physical Sciences Division for the use of meteorology data, and NOAA Global
591 Monitoring Division for the use of balloonsonde data.
592

References

Adgate, J. L., Goldstein, B. D., and McKenzie, L. M.: Potential public health hazards, exposures and health effects from unconventional natural gas development, *Environ. Sci. Technol.*, 48, 8307-8320, 10.1021/es404621d, 2014.

Allen, D. T., Torres, V. M., Thomas, J., Sullivan, D. W., Harrison, M., Hendler, A., Herndon, S. C., Kolb, C. E., Fraser, M. P., Hill, A. D., Lamb, B. K., Miskimins, J., Sawyer, R. F., and Seinfeld, J. H.: Measurements of methane emissions at natural gas production sites in the United States, *P. Natl. Acad. Sci. USA*, 110, 17768-17773, 10.1073/pnas.1304880110, 2013.

Anglada, J. M.: Complex Mechanism of the Gas Phase Reaction between Formic Acid and Hydroxyl Radical. Proton Coupled Electron Transfer versus Radical Hydrogen Abstraction Mechanisms, *Am. Chem. Soc.*, 126, 9809-9820, 10.1021/ja0481169, 2004.

Aschmann, S. M., Arey, J., and Atkinson, R.: Rate Constants for the Reactions of OH Radicals with 1,2,4,5-Tetramethylbenzene, Pentamethylbenzene, 2,4,5-Trimethylbenzaldehyde, 2,4,5-Trimethylphenol, and 3-Methyl-3-hexene-2,5-dione and Products of OH + 1,2,4,5-Tetramethylbenzene, *J. Phys. Chem. A*, 117, 2556-2568, 10.1021/jp400323n, 2013.

Atkinson, R., and Arey, J.: Atmospheric degradation of volatile organic compounds, *Chem. Rev.*, 103, 4605-4638, 2003.

Bates, T. S., Quinn, P. K., Coffman, D. J., Covert, D. S., Miller, T. L., Johnson, J. E., Carmichael, G. R., Uno, I., Guazzotti, S. A., Sodeman, D. A., Prather, K. A., Rivera, M., Russell, L. M., and Merrill, J. T.: Marine boundary layer dust and pollutant transport associated with the passage of a frontal system over eastern Asia, *J. Geophys. Res: Atmos.*, 109, D19S19, 10.1029/2003JD004094, 2004.

Brandt, A. R., Heath, G. A., Kort, E. A., O'Sullivan, F., Pétron, G., Jordaan, S. M., Tans, P., Wilcox, J., Gopstein, A. M., Arent, D., Wofsy, S., Brown, N. J., Bradley, R., Stucky, G. D., Eardley, D., and Harriss, R.: Methane Leaks from North American Natural Gas Systems, *Science*, 343, 733-735, 2014.

Carter, W. P. L., and Seinfeld, J. H.: Winter ozone formation and VOC incremental reactivities in the Upper Green River Basin of Wyoming, *Atmos. Env.*, 50, 255-266, 10.1016/j.atmosenv.2011.12.025, 2012.

Crosson, E. R.: A cavity ring-down analyzer for measuring atmospheric levels of methane, carbon dioxide, and water vapor, *Appl. Phys. B*, 92, 403-408, 10.1007/s00340-008-3135-y, 2008.

de Gouw, J., and Warneke, C.: Measurements of volatile organic compounds in the earth's atmosphere using proton-transfer-reaction mass spectrometry, *Mass. Spectrom. Rev.*, 26, 223-257, 10.1002/mas.20119, 2007.

de Gouw, J. A., Middlebrook, A. M., Warneke, C., Goldan, P. D., Kuster, W. C., Roberts, J. M., Fehsenfeld, F. C., Worsnop, D. R., Canagaratna, M. R., Pszenny, A. A. P., Keene, W. C., Marchewka, M., Bertman, S. B., and Bates, T. S.: Budget of organic carbon in a polluted atmosphere: Results from the New England Air Quality Study in 2002, *J. Geophys. Res.: Atmos.*, 110, D16305, 10.1029/2004JD005623, 2005.

Edwards, P. M., Brown, S. S., Roberts, J. M., Ahmadov, R., Banta, R. M., deGouw, J. A., Dube, W. P., Field, R. A., Flynn, J. H., Gilman, J. B., Graus, M., Helmig, D., Koss, A., Langford, A. O., Lefer, B. L., Lerner, B. M., Li, R., Li, S.-M., McKeen, S. A., Murphy, S. M., Parrish, D. D., Senff, C. J., Soltis, J., Stutz, J., Sweeney, C., Thompson, C. R., Trainer, M. K., Tsai, C., Veres, P. R., Washenfelder, R. A., Warneke, C., Wild, R. J., Young, C. J., Yuan, B., and Zamora, R.: High winter ozone pollution from carbonyl photolysis in an oil and gas basin, *Nature*, 514, 351-354, 10.1038/nature13767, 2014.

Edwards, P. M., Young, C. J., Aikin, K., deGouw, J., Dubé, W. P., Geiger, F., Gilman, J., Helmig, D., Holloway, J. S., Kercher, J., Lerner, B., Martin, R., McLaren, R., Parrish, D. D., Peischl, J., Roberts, J. M., Ryerson, T. B., Thornton, J., Warneke, C., Williams, E. J., and Brown, S. S.: Ozone photochemistry in an oil and natural gas extraction region during winter: simulations of a snow-free season in the Uintah Basin, Utah, *Atmos. Chem. Phys.*, 13, 8955-8971, 10.5194/acp-13-8955-2013, 2013.

Etzkorn, T., Klotz, B., Sørensen, S., Barnes, I., Becker, K. H., and Platt, U.: Gas-phase absorption cross sections of 24 monocyclic aromatic hydrocarbons in the UV and IR spectral ranges, *Atmos. Env.*, 33, 525 - 540, 10.1016/S1352-2310(98)00289-1, 1999.

Gilman, J. B., Burkhardt, J. F., Lerner, B. M., Williams, E. J., Kuster, W. C., Goldan, P. D., Murphy, P. C., Warneke, C., Fowler, C., Montzka, S. A., Miller, B. R., Miller, L., Oltmans, S. J., Ryerson, T. B., Cooper, O. R., Stohl, A., and de Gouw, J. A.: Ozone variability and halogen oxidation within the Arctic and sub-Arctic springtime boundary layer, *Atmos. Chem. Phys.*, 10, 10223-10236, 10.5194/acp-10-10223-2010, 2010.

Gilman, J. B., Lerner, B. M., Kuster, W. C., and de Gouw, J. A.: Source signature of volatile organic compounds from oil and natural gas operations in northeastern Colorado, *Environ. Sci. Technol.*, 47, 1297-1305, 10.1021/es304119a, 2013.

Hard, T. M., Chan, C. Y., Mehrabzadeh, A. A., Pan, W. H., and O'Brien, R. J.: Diurnal cycle of tropospheric OH, *Nature*, 322, 617-620, 1986.

Helmig, D., Thompson, C. R., Evans, J., Boylan, P., Hueber, J., and Park, J. H.: Highly Elevated Atmospheric Levels of Volatile Organic Compounds in the Uintah Basin, Utah, 48, 4707-4715, 10.1021/es405046r, 2014.

Jobson, B. T., Niki, H., Yokouchi, Y., Bottenheim, J., Hopper, F., and Leaitch, R.: Measurements of C2-C6 hydrocarbons during the Polar Sunrise 1992 Experiment: Evidence for Cl atom and Br atom chemistry, *J. Geophys. Res.: Atmos.*, 99, 25355--25368, 10.1029/94JD01243, 1994.

Karion, A., Sweeney, C., Pétron, G., Frost, G., Michael Hardesty, R., Kofler, J., Miller, B. R., Newberger, T., Wolter, S., Banta, R., Brewer, A., Dlugokencky, E., Lang, P., Montzka, S. A., Schnell, R., Tans, P., Trainer, M., Zamora, R., and Conley, S.: Methane emissions estimate from airborne measurements over a western United States natural gas field, *Geophys. Res. Lett.*, 40, 4393-4397, 10.1002/grl.50811, 2013.

Kotamarthi, V. R., and Holdridge, D. J.: Process-scale modeling of elevated wintertime ozone in Wyoming, Argonne National Laboratory, Argonne, IL, 2007.

Kuster, W. C., Jobson, B. T., Karl, T., Riemer, D., Apel, E., Goldan, P. D., and Fehsenfeld, F. C.: Intercomparison of Volatile Organic Carbon Measurement Techniques and Data at La Porte during the TexAQS2000 Air Quality Study, *Environ. Sci. Technol.*, 38, 221-228, 10.1021/es034710r, 2004.

[Li, R., Warneke, C., Graus, M., Field, R., Geiger, F., Veres, P. R., Soltis, J., Li, S.-M., Murphy, S. M., Sweeney, C., Pétron, G., Roberts, J. M., and de Gouw, J.: Measurements of hydrogen sulfide \(H₂S\) using PTR-MS: calibration, humidity dependence, inter-comparison and results from field studies in an oil and gas production region, *Atmos. Meas. Tech.*, 7, 3597-3610, doi:10.5194/amt-7-3597-2014, 2014.](#)

Litovitz, A., Curtright, A., Abramzon, S., Burger, N., and Samaras, C.: Estimation of regional air-quality damages from Marcellus Shale natural gas extraction in Pennsylvania, *Environ. Res. Lett.*, 8, 014017, 10.1088/1748-9326/8/1/014017, 2013.

Lyman, S.: Formaldehyde and Methanol Emission Sources in the Uinta Basin, Uinta Basin Winter Ozone Study 2014 Post Study Technical Meeting, Vernal, UT, 16-17 June 2014.

Martinez, R. D., Buitrago, A. A., Howell, N. W., Hearn, C. H., and Joens, J. A.: The near U.V. absorption spectra of several aliphatic aldehydes and ketones at 300 K, *Atmos. Env.*, 26, 785-792, [http://dx.doi.org/10.1016/0960-1686\(92\)90238-G](http://dx.doi.org/10.1016/0960-1686(92)90238-G), 1992.

McKeen, S. A., Gierczak, T., Burkholder, J. B., Wennberg, P. O., Hanisco, T. F., Keim, E. R., Gao, R. S., Liu, S. C., Ravishankara, A. R., and Fahey, D. W.: The photochemistry of acetone in the upper troposphere: A source of odd-hydrogen radicals, *Geophys. Res. Lett.*, 24, 3177-3180, 10.1029/97gl03349, 1997.

- Miller, S. M., Wofsy, S. C., Michalak, A. M., Kort, E. A., Andrews, A. E., Biraud, S. C., Dlugokencky, E. J., Eluszkiewicz, J., Fischer, M. L., Janssens-Maenhout, G., Miller, B. R., Miller, J. B., Montzka, S. A., Nehrkorn, T., and Sweeney, C.: Anthropogenic emissions of methane in the United States, *P. Natl. Acad. Sci. USA*, 110, 20018-20022, 10.1073/pnas.1314392110, 2013.
- Moore, C. W., Zielinska, B., Pétron, G., and Jackson, R. B.: Air Impacts of Increased Natural Gas Acquisition, Processing, and Use: A Critical Review, *Environ. Sci. Technol.*, 48, 8349-8359, 10.1021/es4053472, 2014.
- Oltmans, S. J., Karion, A., Schnell, R. C., Pétron, G., Sweeney, C., Wolter, S., Neff, D., Montzka, S. A., Miller, B. R., Helmig, D., Johnson, B. J., and Hueber, J.: A high ozone episode in winter 2013 in the Uinta Basin oil and gas region characterized by aircraft measurements, *Atmos. Chem. Phys. Discuss.*, 14, 20117-20157, 10.5194/acpd-14-20117-2014, 2014.
- Roberts, J. M., Fehsenfeld, F. C., Liu, S. C., Bollinger, M. J., Hahn, C., Albritton, D. L., and Sievers, R. E.: Measurements of aromatic hydrocarbon ratios and NO_x concentrations in the rural troposphere: Observation of air mass photochemical aging and NO_x removal, *Atmos. Env.*, 18, 2421-2432, [http://dx.doi.org/10.1016/0004-6981\(84\)90012-X](http://dx.doi.org/10.1016/0004-6981(84)90012-X), 1984.
- Rohrer, F., and Berresheim, H.: Strong correlation between levels of tropospheric hydroxyl radicals and solar ultraviolet radiation, *Nature*, 442, 184-187, 10.1038/nature04924, 2006.
- Schnell, R. C., Oltmans, S. J., Neely, R. R., Endres, M. S., Molenaar, J. V., and White, A. B.: Rapid photochemical production of ozone at high concentrations in a rural site during winter, *Nature Geoscience*, 2, 120-122, 10.1038/ngeo415, 2009.
- Shirley, T. R., Brune, W. H., Ren, X., Mao, J., Leshner, R., Cardenas, B., Volkamer, R., Molina, L. T., Molina, M. J., Lamb, B., Velasco, E., Jobson, T., and Alexander, M.: Atmospheric oxidation in the Mexico City Metropolitan Area (MCMA) during April 2003, *Atmos. Chem. Phys.*, 6, 2753-2765, 10.5194/acp-6-2753-2006, 2006.
- Slusher, D. L., Huey, L. G., Tanner, D. J., Flocke, F. M., and Roberts, J. M.: A thermal dissociation–chemical ionization mass spectrometry (TD-CIMS) technique for the simultaneous measurement of peroxyacyl nitrates and dinitrogen pentoxide, *J. Geophys. Res.: Atmos.*, 109, D19315, 10.1029/2004JD004670, 2004.
- U.S. Energy Information Administration: May 2014 Monthly Energy Review, Washington, DC, 2014.
- Utah Oil and Gas: http://oilgas.ogm.utah.gov/Data_Center/DataCenter.cfm, access: 3 June 2014.
- Warneke, C., Geiger, F., Edwards, P. M., Dube, W., Pétron, G., Kofler, J., Zahn, A., Brown, S. S., Graus, M., Gilman, J. B., Lerner, B. M., Peischl, J., Ryerson, T. B., de Gouw, J. A., and Roberts, J. M.: Volatile organic compound emissions from the oil and natural gas industry in the

Uintah Basin, Utah: oil and gas well pad emissions compared to ambient air composition, Atmos. Chem. Phys., 14, 10977-10988, 10.5194/acp-14-10977-2014, 2014.

Warneke, C., Veres, P., Murphy, S. M., Soltis, J., Field, R. A., Graus, M. G., Koss, A., Li, S.-M., Li, R., Yuan, B., Roberts, J. M., and de Gouw, J. A.: PTR-QMS versus PTR-TOF comparison in a region with oil and natural gas extraction industry in the Uintah Basin in 2013, Atmos.Meas. Tech., 8, 411–420, doi:10.5194/amt-8-411-2015, 2015.

Table 1. Compounds analyzed

PTR-MS	OH rate constant	Average mixing ratio	
Primary compounds	$10^{-12} \text{ cm}^3 \text{ molecule}^{-1} \text{ s}^{-1}$	<i>ppbv (1 σ)</i>	
Benzene	1.22	3.30	(1.92)
Toluene	5.63	4.00	(2.76)
C8 aromatics	16.4 ^a	1.74	(1.36)
C9 aromatics	16.9 ^a	0.365	(0.271)
C10 aromatics	24.2 ^a	0.071	(0.055)
Oxygenated compounds			
<u>Formaldehyde</u>	<u>9.37</u>	<u>3.71</u>	<u>(1.49)</u>
Acetaldehyde	15.0	4.27	(2.39)
2-butanone (MEK)	1.22	2.81	(1.69)
Acetone	0.17	7.97	(4.69)
Formic acid	0.37 ^b	2.56	(1.43)
<u>Compounds with mixed or undetermined source</u>			
Methanol	0.94	44.9	(33.4)
<u>Formaldehyde</u>	<u>9.37</u>	<u>3.71</u>	<u>(1.49)</u>
GC-FID			
Primary compounds			
Ethane	0.248	300	(169)
Propane	1.09	140	(78.6)
<i>n</i> -butane	2.36	48.0	(26.9)
2-methylpropane	2.12	30.3	(17.1)
<i>n</i> -pentane	3.80	18.8	(10.5)
2-methylbutane	3.60	20.9	(11.8)
2,2-dimethylpropane	0.825	0.306	(0.181)
<i>n</i> -hexane	5.20	8.32	(4.65)
Sum of 2- and 3- methylpentane	5.20	6.62	(3.99)
2,2-dimethylbutane	2.23	0.467	(0.294)
Methylcyclopentane	6.90	3.65	(2.27)
<i>n</i> -heptane	6.76	4.00	(2.30)
Methylcyclohexane	9.64	6.74	(4.17)
Ethyne	0.88	0.796	(0.40)
Ethene	8.52	2.05	(1.06)
Propene	26.3	0.171	(0.0724)

^a Rate constants determined in this work.

^b Anglada, 2004.

All other OH rate constants from Atkinson and Arey (2003).

Table 2. Primary compound results

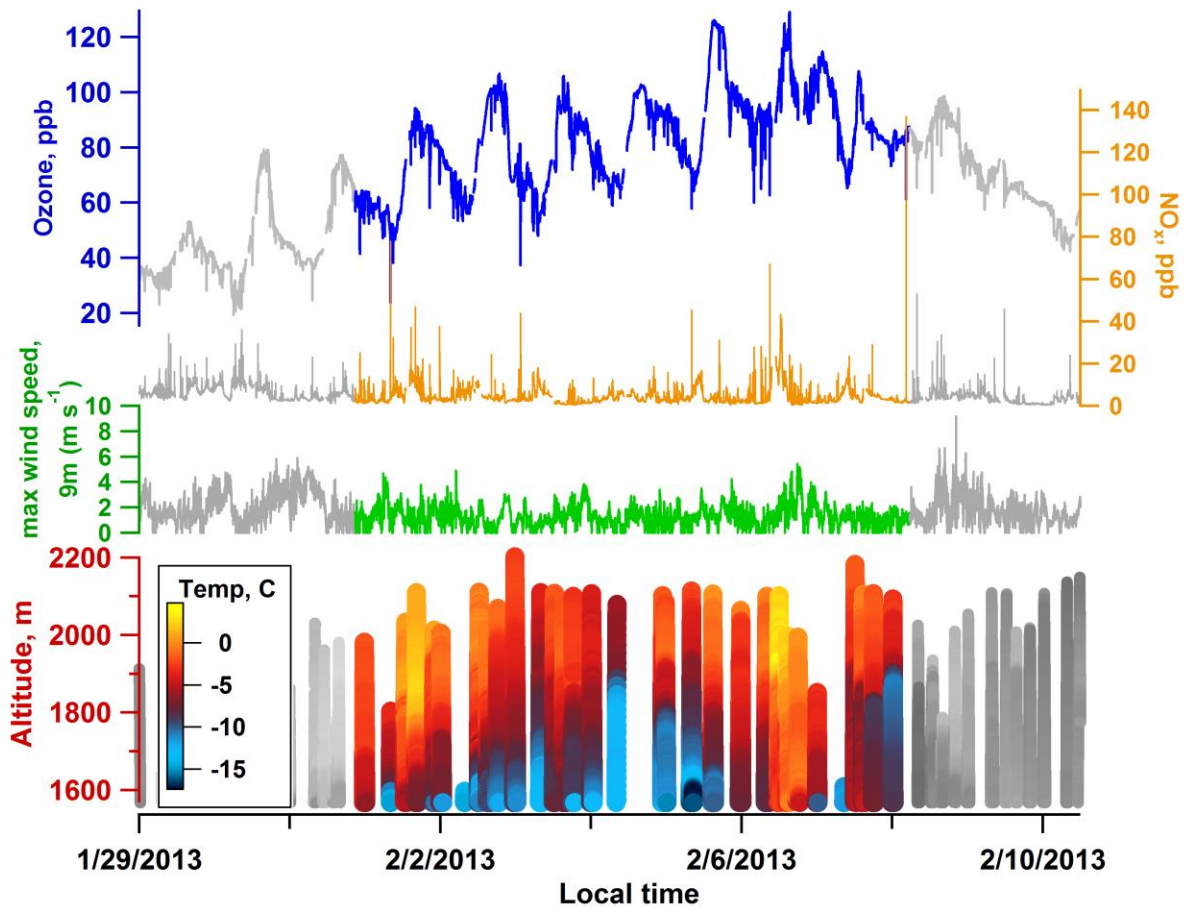
Compound	Emission ratio to benzene by mol	Benzene emission rate 10^5 molecule $\text{cm}^{-3} \text{ s}^{-1}$	[OH] avg. 10^5 molecule cm^{-3}	OH rate constant 10^{-12} cm^3 $\text{molecule}^{-1} \text{ s}^{-1}$	R² – full time series best fit
-----------------	---	--	---	---	--

Toluene	1.5	4.5	2.66	5.63	0.242
C8 aromatics	0.82	4.1	1.86	16.4	0.421
C9 aromatics	0.18	3.9		16.9	0.614
C10 aromatics	0.042	3.8		24.2	0.273

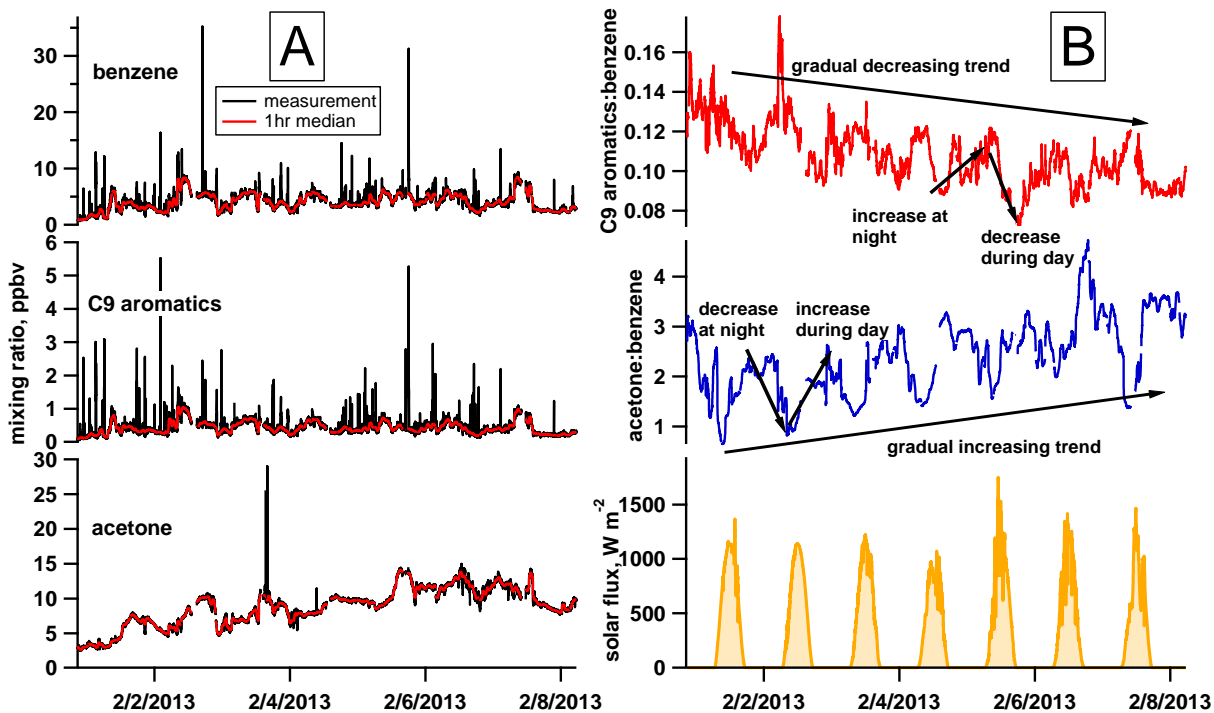
Table 2 includes results from the night-data only best fit (emission ratios, benzene emission rate), and the full time series (including both day and night) best fit ([OH], k_{OH} , and R^2).

Table 3. Oxygenated compound results

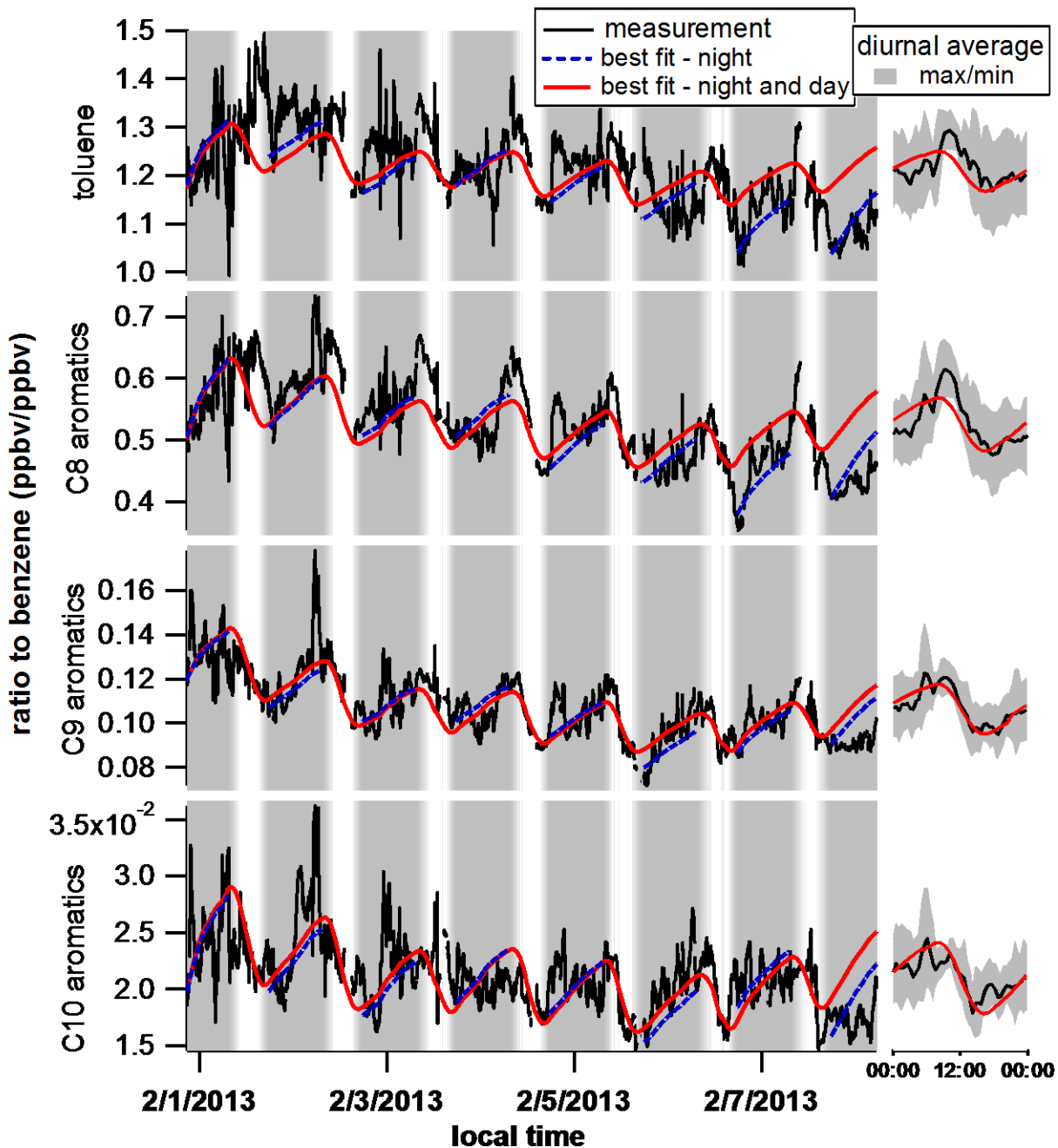
Compound	Benzene emission rate 10^5 molecule $\text{cm}^{-3} \text{ s}^{-1}$	Formation rate constant 10^{-11} cm^3 $\text{molecule}^{-1} \text{ s}^{-1}$	R^2 <i>(daytime</i> <i>data)</i>	Photolysis rate constant s^{-1}
Acetaldehyde	4.91	7.36	0.667	1.2e-6 (Martinez et al., 1992)
Formic acid	6.04	3.30	0.414	1.0e-6 (estimated)
Acetone	4.46	8.72	0.775	5.0e-8 (McKeen et al., 1997)
MEK	4.97	3.42	0.787	3.6e-6 (Martinez et al., 1992)
Methanol	1.34			(day analysis not performed)
Formaldehyde	0.90			(day analysis not performed)



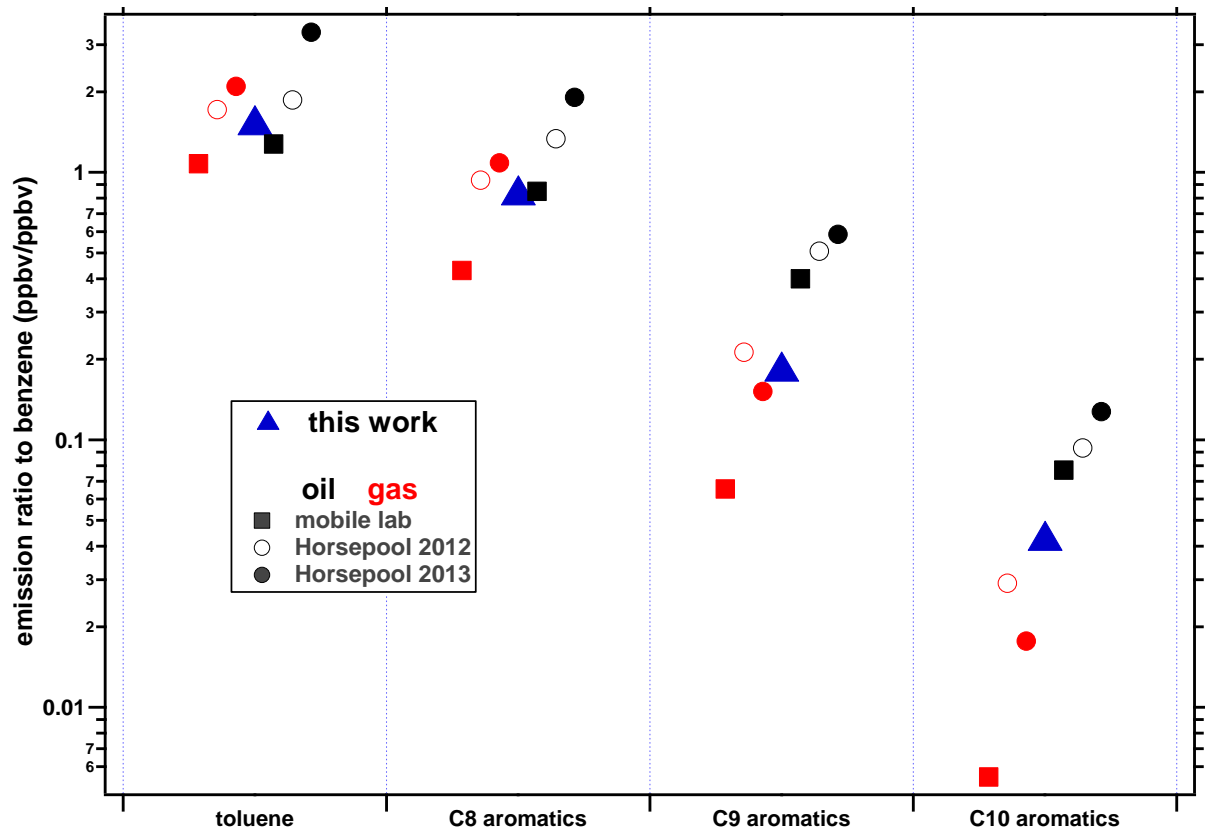
594
 595 Figure 1. Ozone formation event and analysis period selection. The modeled period (colored)
 596 was selected to avoid high wind events on Jan 31 and Feb 8. (center) and include strong
 597 temperature inversions (bottom) to minimize mixing of VOCs in or out of the basin.
 598 Meteorological data courtesy of NOAA Physical Sciences Division. Temperature data from
 599 tethered balloon sonde operated by NOAA Global Monitoring Division.



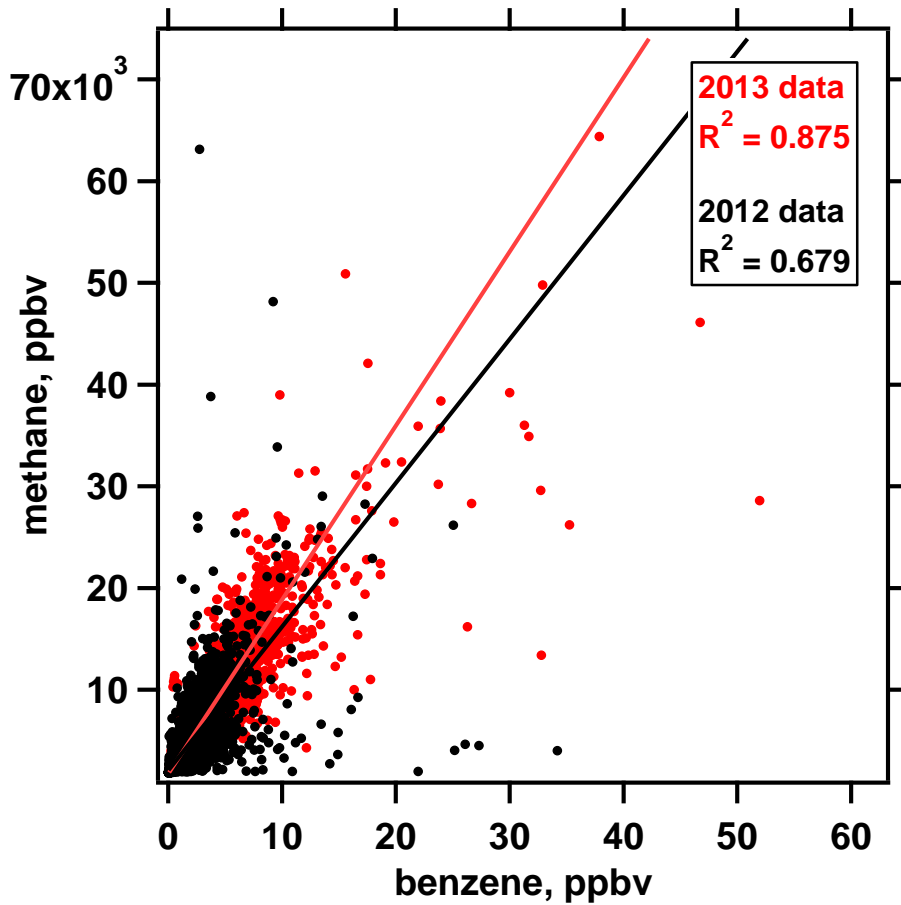
600
 601 Figure 2. Description of trends in VOC concentrations and ratios. (A) Mixing ratios of
 602 benzene, C9 aromatics, and acetone (black), and a one hour running median to isolate
 603 spikes (red). (B) Ratios of C9 aromatics (top) and acetone (center) to benzene. Sunlight
 604 intensity is shown beneath. The spikes visible in panel (A) have been removed to isolate
 605 longer-term trends in VOC behavior (discussed in text).



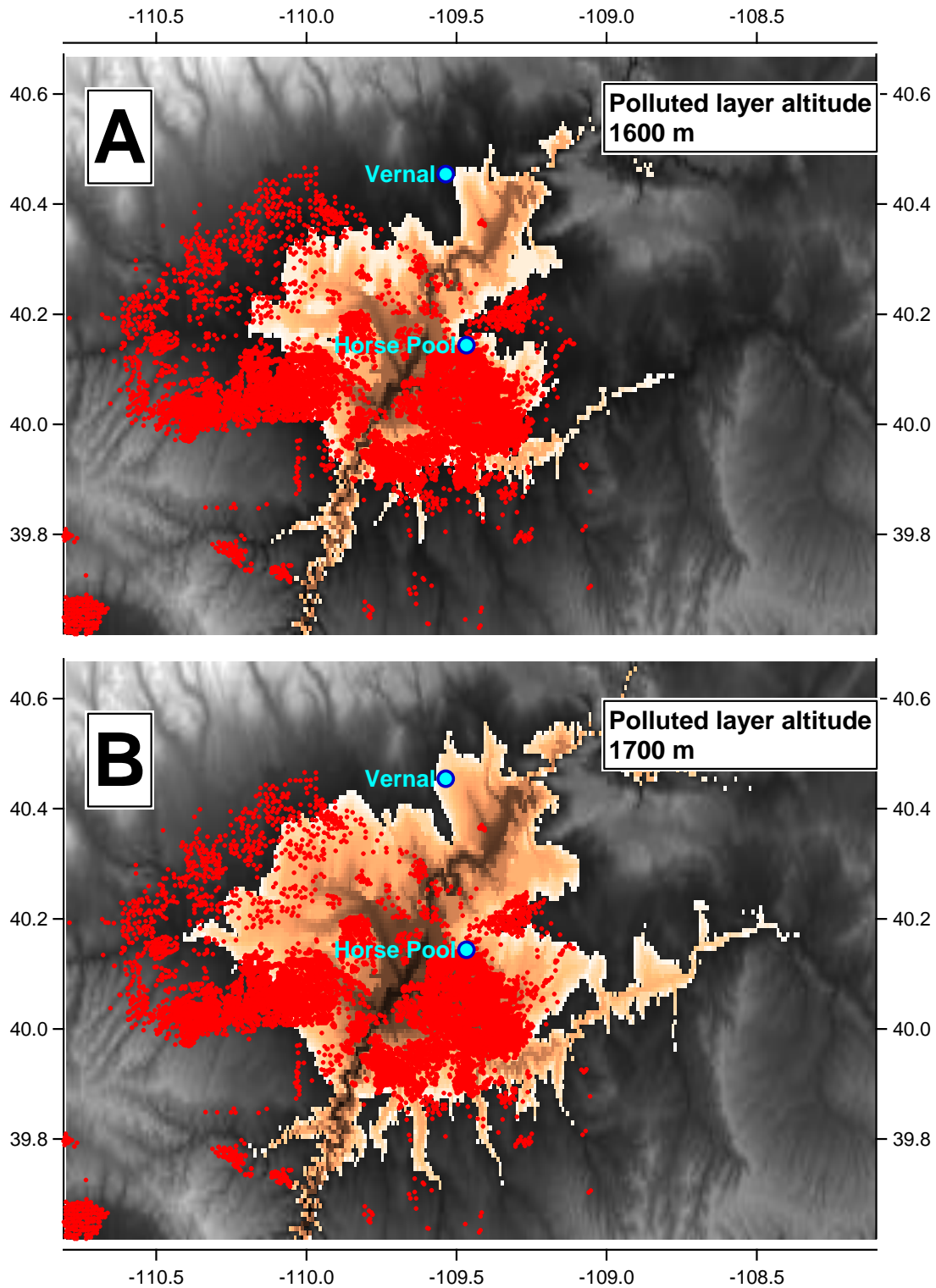
606
 607 Figure 3. Aromatic compound ratios and best fit to night time data (blue) and both night and
 608 day data (red). The background is colored by sunlight intensity to distinguish day and night.
 609 For reproducibility, the initial ratio for each night was chosen from the 10th percentile of
 610 points during the first two hours of evening. In practice, best-fit parameters were largely
 611 insensitive to initial ratio, so long as the selected initial ratio was close to measurements
 612 during the early part of the night. A diurnal average is shown to the right.



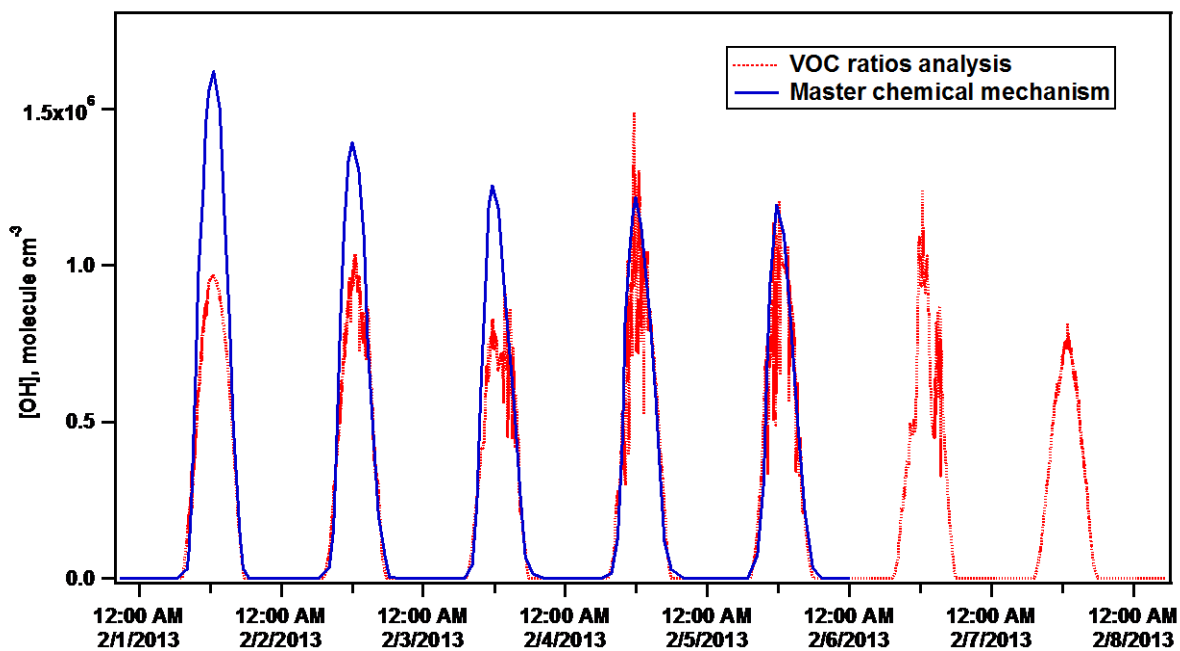
613
 614 Figure 4. Comparison of emission ratio estimates. Emission ratio estimates from this analysis
 615 (blue triangle) give an average emission ratio that is partway between the oil and gas
 616 sources.



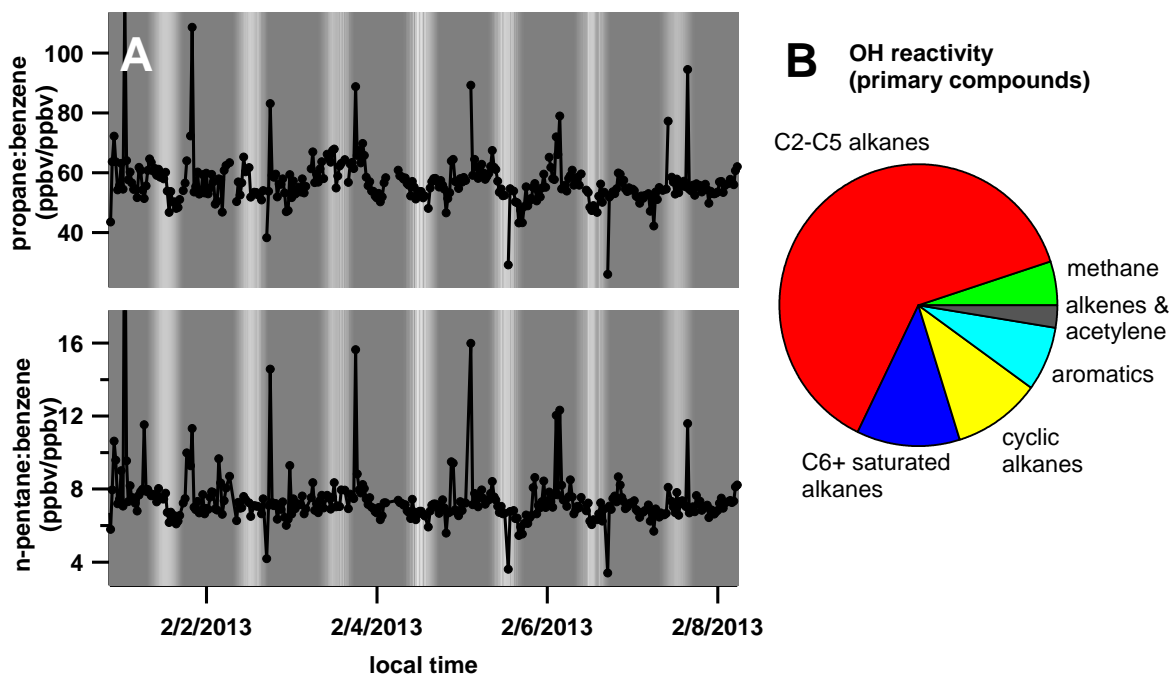
617 Figure 5. Correlation between methane and benzene for all data taken in 2013 (red) and
618 2012 (black).



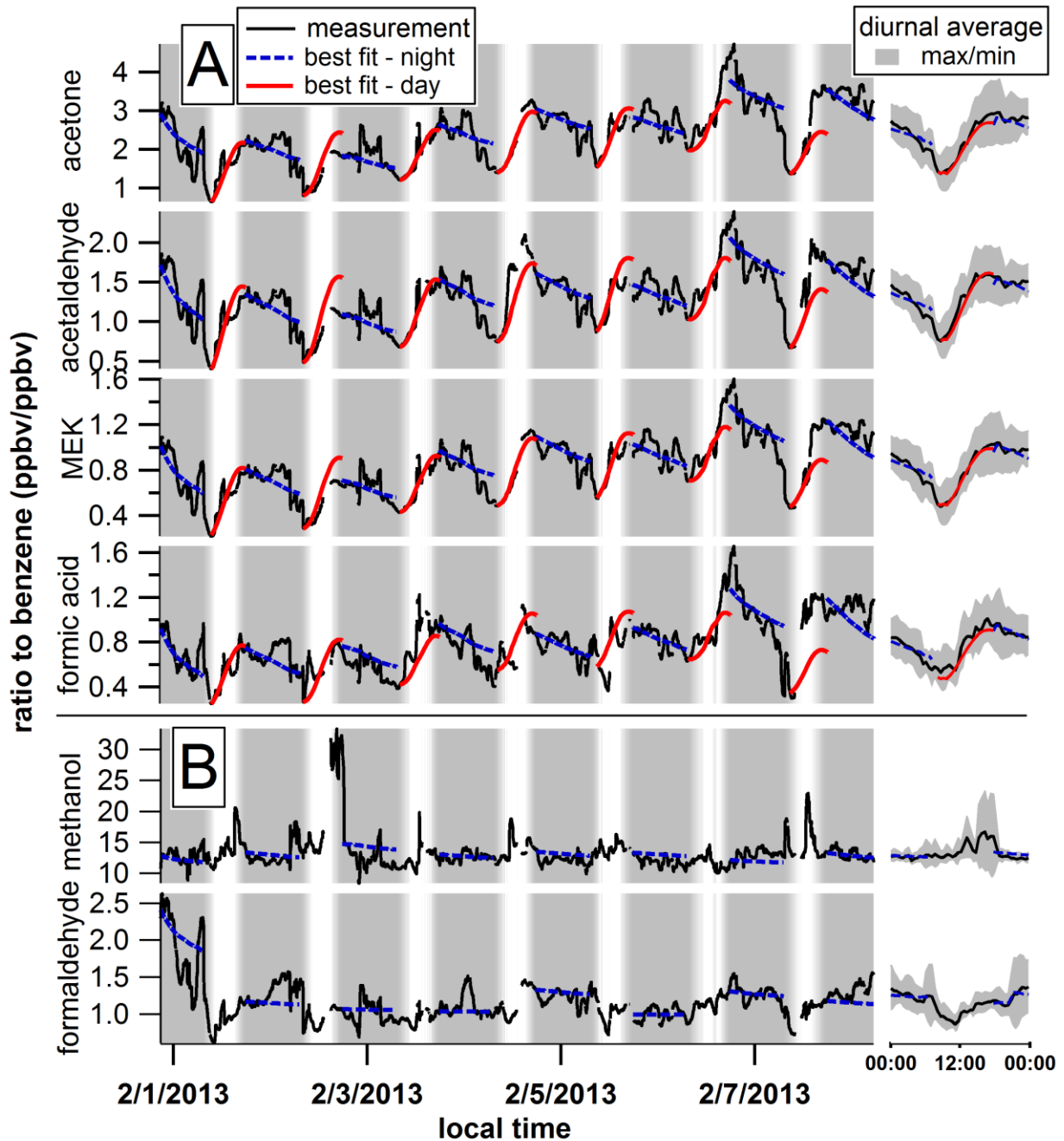
619
 620 Figure 6. Topographical map of the Uintah Basin showing polluted region and well locations.
 621 Total relief is from 1398 meters above sea level to 3627m. The bright (tan) region shows the
 622 area of the polluted region assuming the polluted layer extends to 1600 meters above sea
 623 level (A) or 1700m (B). Locations of producing oil and gas wells are marked in red.



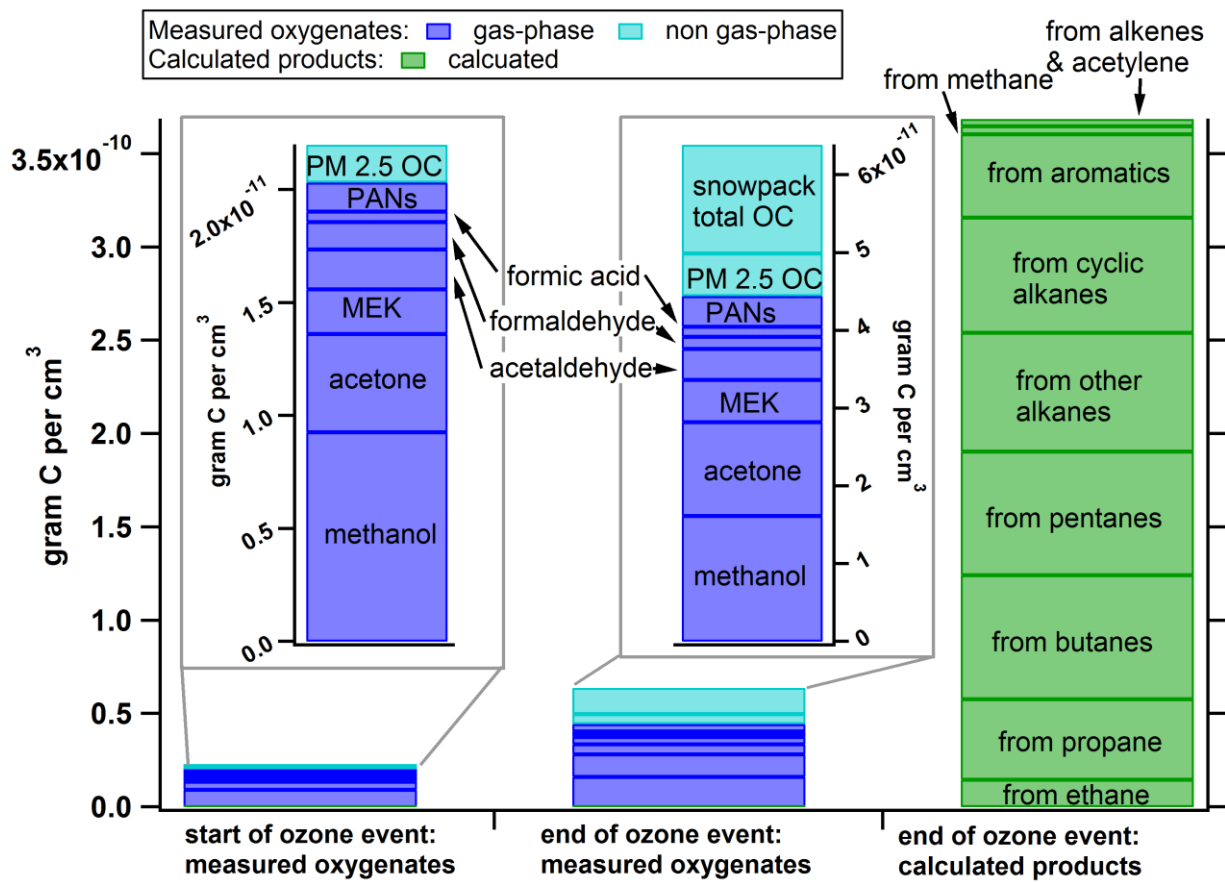
624 Figure 7. Comparison of OH with the Master Chemical Mechanism prediction. There is good
625 agreement between the MCM OH and OH determined from our analysis.



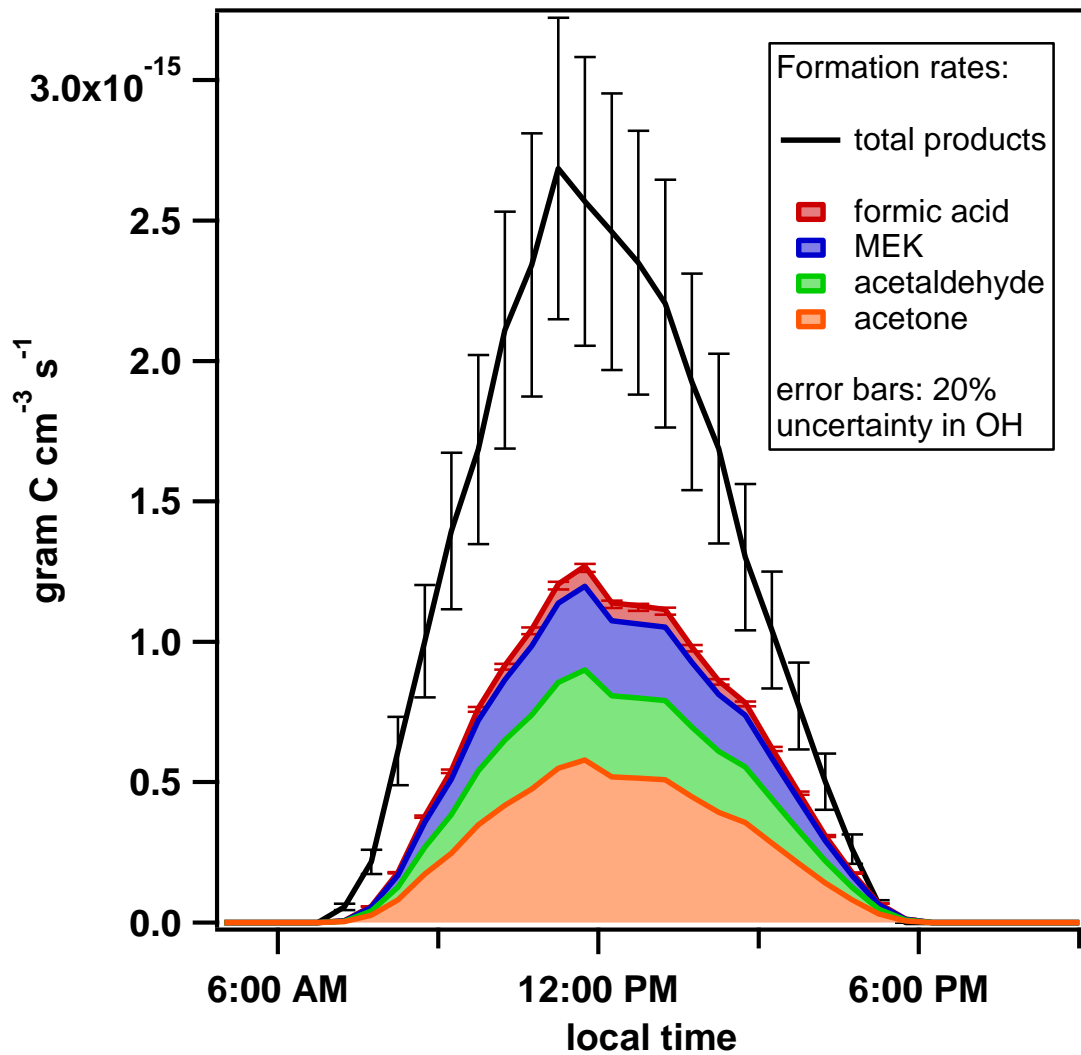
626 Figure 8. A. Because of their slow reaction rates with OH, the ratios of ~~C1~~C2-C5 alkanes to
 627 benzene did not have high diurnal variability and did not change substantially from
 628 beginning to end of the stagnation event (propane and n-pentane measured by GC-FID are
 629 shown as representatives). B. However, because of their high mixing ratios, these species
 630 account for a large fraction (~70%) of primary hydrocarbon-OH reactions.



631 Figure 9. Analysis results for oxygenated compounds. Measured ratio is in black, night best
 632 fit in blue, and day best fit in red. A. The best fit is able to reproduce VOC trends during the
 633 day for acetone, MEK, acetaldehyde, and formic acid. B. The best fit ~~but~~ does not reproduce
 634 night time variability or trends in methanol and formaldehyde, which may have substantial
 635 primary sources uncorrelated with benzene.



636 Figure 10. Organic carbon mass of oxygenated and secondary species. The leftmost two bars
 637 show the carbon mass of secondary species at the beginning (average of first 12 hours) and
 638 end (average of last 12 hours) of the ozone event; speciation is ~~the same in both bars and is~~
 639 detailed in the two insets. Although methanol and formaldehyde may have primary sources,
 640 they are included here in the “product compounds” category to show the maximum
 641 contribution of these species to measured products. The rightmost bar shows the calculated
 642 mass of secondary compounds at the end of the ozone event; within this bar, the contribution
 643 from each precursor is delineated.



644 Figure 11. Comparison of total product formation rates (black) and measured carbonyl
 645 formation rates. There is a substantial gap that indicates the formation of other oxidation
 646 products.